

An experimental comparison of the relative benefits of work and torque assistance in ankle exoskeletons

Rachel W. Jackson¹ and Steven H. Collins^{1,2}

¹Department of Mechanical Engineering, Carnegie Mellon University, Pittsburgh, Pennsylvania; and ²Robotics Institute, Carnegie Mellon University, Pittsburgh, Pennsylvania

Submitted 19 December 2014; accepted in final form 2 July 2015

Jackson RW, Collins SH. An experimental comparison of the relative benefits of work and torque assistance in ankle exoskeletons. *J Appl Physiol* 119: 541–557, 2015. First published July 9, 2015; doi:10.1152/jappphysiol.01133.2014.—Techniques proposed for assisting locomotion with exoskeletons have often included a combination of active work input and passive torque support, but the physiological effects of different assistance techniques remain unclear. We performed an experiment to study the independent effects of net exoskeleton work and average exoskeleton torque on human locomotion. Subjects wore a unilateral ankle exoskeleton and walked on a treadmill at 1.25 m·s⁻¹ while net exoskeleton work rate was systematically varied from -0.054 to 0.25 J·kg⁻¹·s⁻¹, with constant (0.12 N·m·kg⁻¹) average exoskeleton torque, and while average exoskeleton torque was systematically varied from approximately zero to 0.18 N·m·kg⁻¹, with approximately zero net exoskeleton work. We measured metabolic rate, center-of-mass mechanics, joint mechanics, and muscle activity. Both techniques reduced effort-related measures at the assisted ankle, but this form of work input reduced metabolic cost (-17% with maximum net work input) while this form of torque support increased metabolic cost (+13% with maximum average torque). Disparate effects on metabolic rate seem to be due to cascading effects on whole body coordination, particularly related to assisted ankle muscle dynamics and the effects of trailing ankle behavior on leading leg mechanics during double support. It would be difficult to predict these results using simple walking models without muscles or musculoskeletal models that assume fixed kinematics or kinetics. Data from this experiment can be used to improve predictive models of human neuromuscular adaptation and guide the design of assistive devices.

biomechanics; locomotion; ankle foot orthosis; gait; rehabilitation

EXOSKELETONS ACT IN PARALLEL with the human body and augment, rather than replace, the assisted joints. Assisting human locomotion with exoskeletons therefore requires consideration of both biological and exoskeleton contributions to assisted joint mechanics. When an exoskeleton is added to a human user, the human must adapt to a novel environment and discover new control strategies, complicating the task of determining useful assistance techniques. Performing human experiments with exoskeletons can help us understand how to best interact with the human user and may provide insights into fundamental principles governing locomotor coordination and adaptation (19).

Simulations, prior experiments, and intuition can be helpful in deciding what assistance techniques are worth exploring. Simple walking models and related experiments suggest that the trailing leg performs positive work around the step-to-step

transition to help redirect the velocity of the body center of mass and compensate for energy lost during leading leg collision (14, 22, 29, 38). Nearly all of this push-off work is performed at the ankle joint (34, 53), and musculoskeletal simulations suggest that ankle plantarflexor muscles involved in push-off consume ~27% of the metabolic energy of walking (49). Replacing part of this biological work with external mechanical work, via an exoskeleton acting in parallel with the ankle joint, may reduce force and work of the plantarflexor muscles and decrease overall metabolic energy consumption. Alternatively, increasing total ankle joint work, by augmenting rather than replacing biological ankle joint work, could reduce metabolic energy consumed elsewhere in the body. Other studies and musculoskeletal models of human walking suggest that there is also a significant metabolic cost associated with generating muscle force to support body weight (23, 24, 37, 47). Providing exoskeleton torques in parallel with the biological ankle joint, without supplying any net mechanical work, could reduce plantarflexor muscle forces required to support body weight and reduce associated energy consumption.

Although exoskeleton work and torque assistance approaches are well-motivated, they have not been thoroughly tested. Many isolated exoskeleton experiments have been conducted, but comparisons between assistance techniques have often been confounded by factors other than device behavior, such as device mass, differences in study protocols, or covariation of other possibly influential parameters. Furthermore, complete biomechanical measurements have rarely been obtained. It therefore remains uncertain how different types of assistance impact whole body coordination. An experiment that uses an exoskeleton to compare the effects of work input and torque support on locomotor mechanics and energetics could help us understand the independent benefits of each assistance technique and could provide insights into the independent costs of performing work and producing force with muscles. Such a study was previously recommended by Sawicki and Ferris (41).

Distinguishing between the relative effectiveness of work and torque assistance is important because these strategies have disparate implications for device design. Providing net positive mechanical work with an exoskeleton requires an actuator system, such as an electric motor and battery, which adds distal mass, potentially offsetting energy reductions (5). External supporting torques can be achieved with lightweight, elastic mechanisms, such as springs (11), but these unpowered devices cannot deliver net work to the user. In both cases some amount of control can be performed cheaply, for example, by embedded microprocessors and small clutches (10, 52), making the amount of net work provided over a cycle the primary distinction between approaches. Some combination of work and

Address for reprint requests and other correspondence: S. H. Collins, Carnegie Mellon Univ., Mechanical Engineering, Scaife Hall 316, 5000 Forbes Ave., Pittsburgh, PA 15213 (e-mail: stevecollins@cmu.edu).

torque is likely to be optimal, but understanding how each independently affects the human user would facilitate a more effective design process.

Using musculoskeletal models to gain insights into fundamental locomotor control and to predict the human response to untested assistance strategies is an appealing alternative to human experiments. These simulations allow for a large number and variety of tests to be run quickly and full body measurements to be obtained. Generating accurate predictions, however, is a challenging problem due to the complexity and redundancy of the human neuromuscular system. For example, researchers using biomechanics measurements taken after patient adaptation still find it difficult to accurately estimate experimentally measured *in vivo* knee contact forces (20). Rich data sets obtained through controlled human experiments, like those mentioned in Ref. 20, provide information about the human response to novel interventions and help improve predictive musculoskeletal models.

Our goal was to conduct a controlled experiment comparing the effects of a particular mode of work input and torque support assistance on human mechanics and energetics. Increased exoskeleton work was expected to reduce the metabolic energy cost associated with work input to redirect the body's center-of-mass velocity, appearing as reduced work at the assisted ankle joint and reduced biological contributions to center-of-mass work overall. Increased exoskeleton torque was expected to reduce the metabolic energy cost associated with supporting body weight, appearing as reductions in assisted ankle torque and associated muscle activity. Regardless of the outcomes, we expected the biomechanics and muscle activity data set obtained from this experiment to provide insights into why different assistance strategies are more effective than others, inform future device designs, and provide validation data for predictive models.

METHODS

We conducted an experiment in which we compared the independent effects of one form of exoskeleton work input and torque support on human energetics, mechanics, and muscle activity during walking. We applied a wide range of net work and average torque values using an ankle exoskeleton worn by healthy subjects on one leg as they walked on a treadmill and compared changes within and across the two assistance techniques.

Ankle Exoskeleton Emulator

Work and torque were applied by a high-performance, tethered ankle exoskeleton. A lightweight instrumented frame (Fig. 1, A and B), worn on the foot and shank, was connected to an off-board motor via a flexible Bowden cable transmission (7, 54). The ankle exoskeleton weighed 0.826 kg and was attached to a shoe. Forces were applied to the human at the shank, toe, and heel, resulting in maximum plantarflexor torques of up to $120 \text{ N}\cdot\text{m}^{-1}$ (9). A load cell (LC201 Series; OMEGA Engineering, Stamford, CT) in series with the transmission at the ankle joint measured torques with a maximum of 1% error after calibration. Fiberglass leaf springs provided series compliance and improved regulation of joint torque (58). The exoskeleton joint angle was measured with an optical encoder (E8P; US Digital, Vancouver, WA). The axis of rotation of the exoskeleton was aligned so as to intersect the medial malleolus of the ankle of the human user. A foot switch (McMaster-Carr, Aurora, OH) in the heel of the shoe was used to detect heel strike.

Exoskeleton Control

Exoskeleton work and torque were regulated using control of motor position in time with iterative learning. We used a series elastic actuation approach, in which differences between motor position and ankle joint position stretched a series spring, giving rise to torques approximated by:

$$\tau_a \approx k \cdot (\theta_m \cdot R^{-1} - \theta_a) \quad (1)$$

where τ_a is the exoskeleton ankle joint torque; k is the series stiffness, which had a maximum value of $\sim 130 \text{ N}\cdot\text{m}\cdot\text{rad}^{-1}$ but varied greatly due to friction in the transmission and other nonlinearities in the system; θ_m is the motor angle; θ_a is the exoskeleton ankle joint angle, approximately equal to the human ankle joint angle; and R is the gear ratio between the motor and exoskeleton ankle joint, which was 18.5 in this study. (Note that measurements of joint torque were made using a load cell.)

We utilized dynamic interactions between the exoskeleton and human to generate desired plantarflexor torque and power over time. We defined a piece-wise linear desired motor position trajectory for each torque and work combination (Fig. 2). The first node of this trajectory (θ_1) corresponded with 0% stride and was equal to the measured ankle angle at heel strike. The final node (θ_4) was reached at 60% of stride and was approximately equal to the ankle angle at toe-off. The second and third nodes (θ_2 and θ_3) were reached at 36 and 48% of stride, which we estimated would approximately independently affect exoskeleton torque and work, respectively, due to differences in joint velocity at those instants.

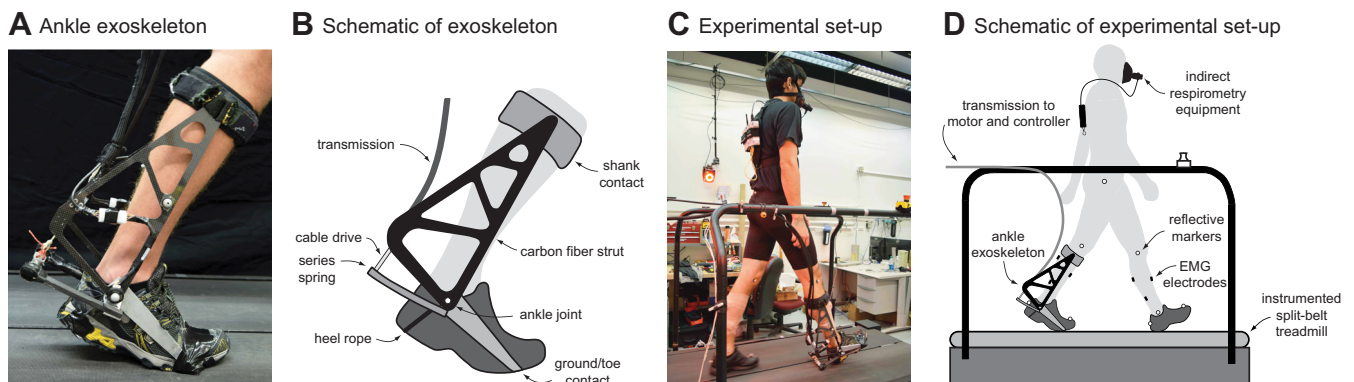


Fig. 1. Custom-designed ankle exoskeleton and experimental setup. A: photograph of ankle exoskeleton used to apply plantarflexor torques. B: schematic of exoskeleton highlighting key components. C: photograph of experimental setup. D: schematic of experimental setup highlighting key components. Metabolic energy consumption, segment kinematics, ground reaction forces, muscle activity, and exoskeleton mechanics were measured.

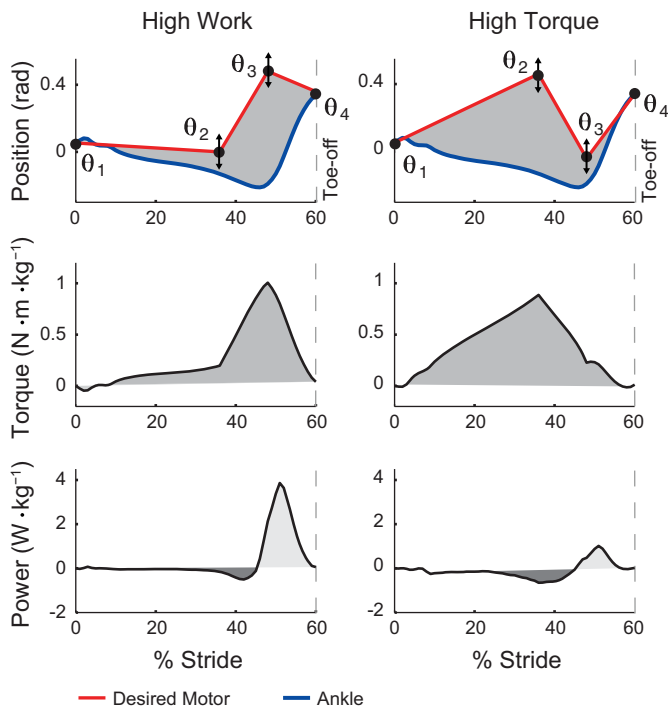


Fig. 2. Ankle exoskeleton control illustration. *Top row:* desired motor angle was defined by 4 nodes in time. Differences between motor angle and ankle angle (blue) stretched a series spring, generating joint torques. The middle two nodes, θ_2 and θ_3 , were iteratively updated to maintain desired average torque and net work rate. *Middle row:* resulting exoskeleton ankle joint torque in time. *Bottom row:* resulting exoskeleton ankle power in time. *Left column:* illustration of a motor trajectory that would result in medium average torque and high net work. *Right column:* trajectory that would result in high average torque and zero net work.

The resulting exoskeleton torque and work were measured in real time on each stride using the load cell and joint encoder. A stride was defined as heel strike to heel strike of the exoskeleton-side leg. Average exoskeleton torque was defined as the integral of measured torque over a stride divided by stride duration. Exoskeleton ankle joint velocity was computed as the discrete derivative of measured exoskeleton ankle angle and low-pass filtered with a cutoff frequency of 50 Hz. Exoskeleton power was calculated by multiplying joint torque by joint velocity. The net exoskeleton work rate was defined as the integral of power over a stride, divided by stride duration. Negative power phases therefore reduced net work rate. This definition of net work rate is equivalent to average power.

We implemented an iterative learning scheme to maintain desired average exoskeleton torque and work rate, which compensated for changes in human kinematics over time. This approach is conceptually similar to an online version of the controller described in Ref. 27. On each stride, θ_2 and θ_3 were changed in a way expected to reduce errors between desired and measured torque and work on the subsequent stride:

$$\theta_2(n+1) = \theta_2(n) - k_2 \cdot e_{\text{tau}}(n) \quad (2)$$

$$\theta_3(n+1) = \theta_3(n) - k_3 \cdot e_{\text{wrk}}(n) \quad (3)$$

where $\theta_2(n+1)$ and $\theta_3(n+1)$ are the motor positions of the second and third nodes, respectively, on the $(n+1)^{\text{th}}$ stride; $\theta_2(n)$ and $\theta_3(n)$ are the motor positions of the second and third nodes, respectively, on the n^{th} stride; $e_{\text{tau}}(n)$ is the error in average torque for the n^{th} stride; $e_{\text{wrk}}(n)$ is the error in net work rate for the n^{th} stride; and k_2 and k_3 are iterative learning gains. Changes in node values were made at exoskeleton heel strike, i.e., at the end of the n^{th} stride and the beginning

of the $(n+1)^{\text{th}}$ stride. Gains were manually tuned during pilot testing to minimize error while maintaining stability, which resulted in values of $k_2 = 3 \cdot 10^{-4} \text{ rad} \cdot (\text{N} \cdot \text{m})^{-1}$ and $k_3 = 3 \cdot 10^{-4} \text{ rad} \cdot (\text{J} \cdot \text{s}^{-1})^{-1}$.

Experimental Protocol

We independently varied net exoskeleton work rate and average exoskeleton torque in one-dimensional parameter studies referred to here as the Work Study and Torque Study, respectively. In the Work Study, we applied five conditions referred to as Negative Work, Zero Work, Low Work, Medium Work, and High Work, in which desired net exoskeleton work rate ranged from about -50 to 250% of net ankle work rate observed during normal walking and desired average torque was $\sim 25\%$ of the value observed during normal walking (10). In the Torque Study, we applied four conditions referred to as Zero Torque, Low Torque, Medium Torque, and High Torque, in which desired average exoskeleton torque ranged from about 0 to 40% of the value observed during normal walking and desired net work rate was approximately zero. Parameters in the Zero Work and Medium Torque conditions were identical, so we tested this condition once.

Subjects walked on a treadmill at $1.25 \text{ m} \cdot \text{s}^{-1}$ for 8 min while wearing the exoskeleton on one leg for each study condition (Fig. 1, C and D). Subjects also completed Quiet Standing and Normal Walking trials in street shoes, which lasted 3 and 6 min, respectively. Subjects completed one training day in addition to the collection day. On the training day, subjects were exposed to each condition in a particular order: first in order of increasing average exoskeleton torque and then in order of increasing net exoskeleton work. Subjects were given verbal coaching to “try relaxing your ankle muscles” and “try not to resist the device.” On the collection day, all conditions were presented in random order.

Eight healthy, able-bodied participants ($n = 8$, 7 men and 1 woman; age = 25.1 ± 5.1 yr; body mass = 77.5 ± 5.6 kg; leg length = 0.89 ± 0.03 m) were included in the study. All subjects provided written informed consent before completing the protocol, which was approved by the Carnegie Mellon Institutional Review Board. Data from a 9th and 10th subject were excluded as outliers; a large portion of metabolic rate data for these subjects was more than two standard deviations (2σ) from the study mean and this skewed the average data away from a normal distribution. Two additional recruits were unable to complete all conditions during training, due to difficulty adapting to exoskeleton behavior and did not progress to the collection day.

Measured Outcomes

Metabolic rate. Metabolic rate was estimated using indirect calorimetry. Volumetric oxygen consumption and carbon dioxide expulsion rates were measured using wireless, portable metabolics equipment (Oxycon Mobile; CareFusion, San Diego, CA). Data from the last 3 min of each trial were averaged and substituted into a widely used equation (4) to calculate metabolic rate. Net metabolic rate was calculated by subtracting metabolic power during Quiet Standing from the different walking conditions. Change in metabolic rate for the Work Study was calculated by subtracting the metabolic power during the Zero Work condition from metabolic power during the five Work Study conditions. Change in metabolic rate for the Torque Study was calculated by subtracting the metabolic power during the Zero Torque condition from metabolic power during the four Torque Study conditions. Metabolic rate was normalized to body mass.

Center-of-mass mechanics. We approximated center-of-mass work rates for the right and left legs using the individual limbs method (15). Ground reaction forces were sampled at a frequency of 2,000 Hz using an instrumented split-belt treadmill (Bertec, Columbus, OH). Three-dimensional center-of-mass acceleration was calculated by summing right and left ground reaction forces and dividing by body mass. Integration of center-of-mass acceleration over a stride resulted in an approximation of center-of-mass velocity in time. Constants of integration were selected such that average center-of-mass velocity

equaled that of the treadmill in the fore-aft direction ($1.25 \text{ m}\cdot\text{s}^{-1}$) and zero in the medio-lateral and superior-inferior directions over an average stride. We took the dot product of center-of-mass velocity and the right and left ground reaction force to obtain center-of-mass power in time for the right and left leg, respectively. We calculated work rate during the collision, rebound, preload, and push-off phases of the stance period (15).

Joint mechanics. We used inverse kinematics and dynamics analyses to approximate joint-level mechanics. Reflective markers were placed on the sacrum, left and right anterior superior iliac spine, greater trochanter, medial and lateral epicondyles of the knee, medial and lateral malleoli of the ankle, third metatarsophalangeal joint of the toe, and posterior calcaneus of the heel. Three-dimensional marker positions were recorded using a seven camera motion capture system at a rate of 100 Hz (MX Series; Vicon Motion Systems, Oxford, UK). We used published anthropometric data (12, 16) to estimate limb masses and rotational inertias. We calculated joint velocities, accelerations, torques, and powers using inverse dynamics analysis (53) of ground reaction forces, joint positions, and estimated segment properties. We calculated joint work rate for features of interest as the integral of joint power over that period of positive or negative work (based on features defined by Ref. 53) divided by the stride period. Exoskeleton-side biological ankle mechanics were calculated by subtracting measured exoskeleton mechanics from total, inverse-dynamics-derived exoskeleton-side ankle mechanics.

Muscle activity. We measured lower-limb muscle activity using surface electromyography. Wireless electrodes were placed on the medial and lateral aspects of the soleus, medial and lateral gastrocnemius, tibialis anterior, vastus medialis, biceps femoris, and rectus femoris on both legs and sampled at a frequency of 2,000 Hz (Trigno Wireless System; Delsys, Boston, MA). Each signal was high-pass filtered with a cutoff frequency of 20 Hz, rectified, and low-pass filtered with a cutoff frequency of 6 Hz in postprocessing (18). Erroneous signals for 144 individual muscles on individual trials ($\sim 12\%$ of all electromyographic data) were discarded from the averaged data set. In some cases errors were due to a faulty sensor. In other cases, identified by visual inspection of the measured pattern, errors seem to have been due to poor electrode connectivity. Electromyographic signals for each condition were normalized to average peak activation during Normal Walking. If measured muscle activity for Normal Walking was erroneous, electromyographic signals across conditions were normalized to average peak activation during the Zero Torque condition, in which the exoskeleton did not apply torques. Root-mean-square values of measured electromyography were computed and used to compare muscle activity across conditions.

Normalization and statistical analysis. We compared metabolic rate, center-of-mass mechanics, joint mechanics, and muscle activity across conditions. Average trajectories, normalized to percent stride, were generated for each subject. Metabolic rate, center-of-mass mechanics, and joint mechanics were normalized to body mass, while muscle activity measurements were normalized to average peak activation during Normal Walking. Scalar outcomes were obtained by taking the integral of the average trajectory and dividing by average stride time. Some of the resulting measurements have units of watts per kilogram, which we present as $\text{J}\cdot\text{kg}^{-1}\cdot\text{s}^{-1}$ so as to distinguish work divided by stride time from instantaneous power. All outcomes were averaged across subjects. Standard deviations represent variations between subjects.

For the Work Study, all pair-wise statistical comparisons were made with respect to the Zero Work condition. For the Torque Study, all pair-wise statistical comparisons were made with respect to the Zero Torque condition. We first performed a repeated-measures ANOVA to test for trend significance in each outcome. On measures that showed significant trends, we performed paired *t*-tests to compare conditions. We then applied the Holm-Šidák step-down correction for multiple comparisons (21) and used a significance level of $\alpha = 0.05$.

RESULTS

As applied in this study, increasing net exoskeleton work reduced metabolic energy consumption, while increasing average exoskeleton torque increased metabolic energy consumption. Both assistance techniques decreased effort-related measures at the exoskeleton-side biological ankle. With increasing exoskeleton work, however, total exoskeleton-side ankle work and center-of-mass push-off increased and contralateral-limb collision and rebound decreased, with concomitant decreases in contralateral-limb knee work, torque, and vastus muscle activity. Increasing exoskeleton torque had the opposite effects.

Exoskeleton Work and Torque

The exoskeleton applied a wide range of values of net joint work and average joint torque across conditions (Fig. 3). In the Work Study, net exoskeleton work divided by stride time (work rate) increased from the Negative Work condition to the Zero Work condition ($P = 2\cdot 10^{-7}$) and from the Zero Work condition to the High Work condition ($P = 1\cdot 10^{-7}$; Fig. 4). Across Work Study conditions, average exoskeleton torque was always within 13% of the value in the Zero Work condition. In the Torque Study, average exoskeleton torque increased from the Zero Torque condition to the High Torque condition ($P = 5\cdot 10^{-8}$). Across Torque Study conditions, there was a trend towards reduced net work rate with increasing average torque (ANOVA, $P = 2\cdot 10^{-4}$), but the work rate was always within $0.015 \pm 0.005 \text{ J}\cdot\text{kg}^{-1}\cdot\text{s}^{-1}$ of zero, or 6% of the maximum value in the Work Study.

Metabolics

Metabolic energy consumption was reduced with increasing net exoskeleton work rate but increased with increasing average exoskeleton torque. Metabolic rate decreased by 17% from the Zero Work condition to the High Work condition ($P = 2\cdot 10^{-4}$; Fig. 5, A and B). With the use of least-squares linear

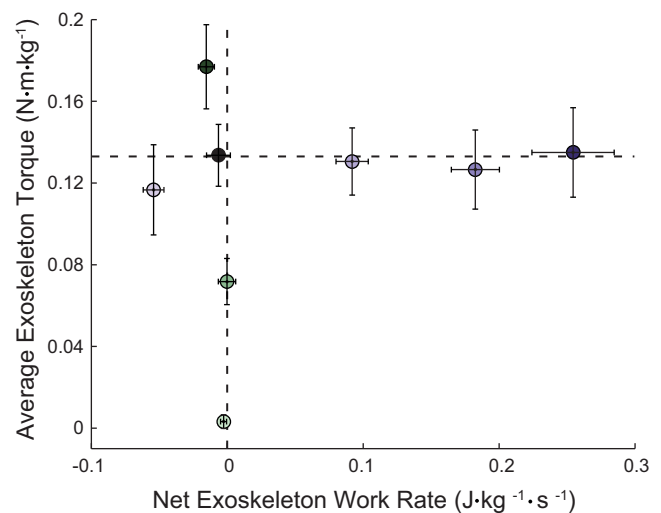


Fig. 3. Average torque vs. net work rate measured for each exoskeleton condition. Work Study is in purple and Torque Study is in green, with darker colors indicating higher values. Dots are mean values and whiskers indicate SDs associated with intersubject variability.

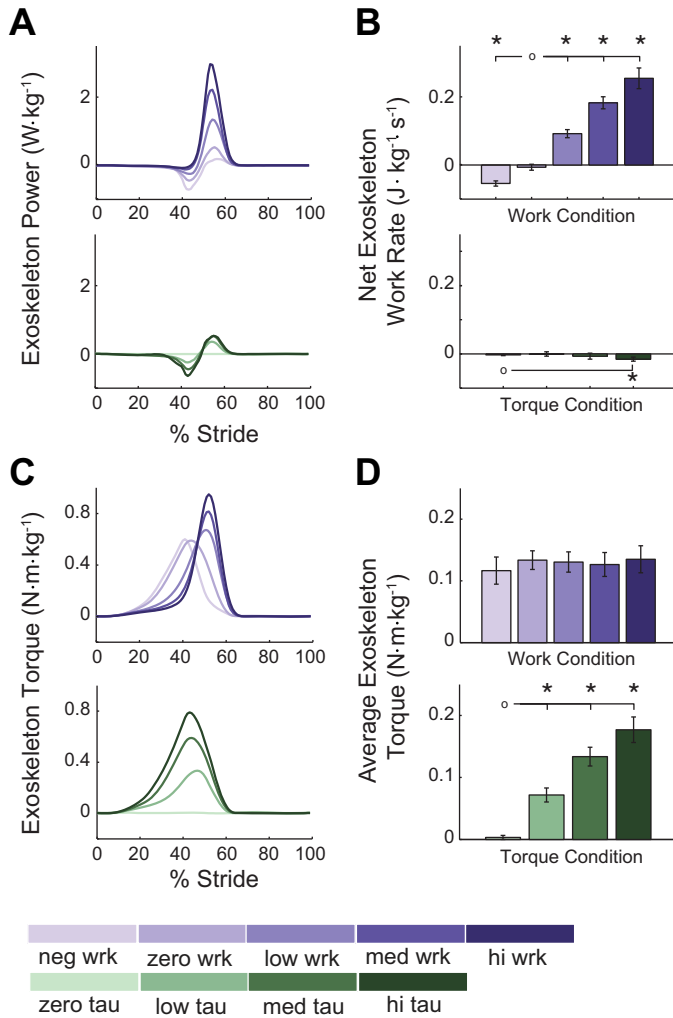


Fig. 4. Applied exoskeleton net work rate and average torque varied widely across conditions. In the Work Study, exoskeleton power (A) and net work rate (B) increased across conditions by shifting the exoskeleton torque profile (C) but maintaining consistent average torque (D). In the Torque Study, net work rate was approximately zero, while average torque increased across conditions. Work Study is in purple and Torque Study is in green, with darker colors indicating higher values. Curves are study average trajectories. Bars and whiskers are means \pm SD of subject-wise integrations of corresponding curves. *Statistical significance with respect to the conditions designated by open circles.

regression, the best fit line relating the change in metabolic rate, P_{met} , to net exoskeleton work rate, W_{exo} , was found to be $P_{met} \approx -2.52 \cdot W_{exo}$ ($R^2 = 0.6$, $P = 2 \cdot 10^{-8}$). By contrast, metabolic rate increased by 13% from the Zero Torque condition to the High Torque condition ($P = 1 \cdot 10^{-3}$; Fig. 5, C and D). The best fit line relating change in metabolic rate, P_{met} , to average exoskeleton torque, τ_{exo} , was found to be $P_{met} \approx 2.45 \cdot \tau_{exo}$ ($R^2 = 0.3$, $P = 2 \cdot 10^{-3}$). The large error bars observed in the metabolic data are a result of intersubject variability.

Exoskeleton-Side Ankle Mechanics

Both modes of assistance reduced biological components of work, torque, and plantarflexor muscle activity at the assisted ankle joint. Positive biological ankle work rate

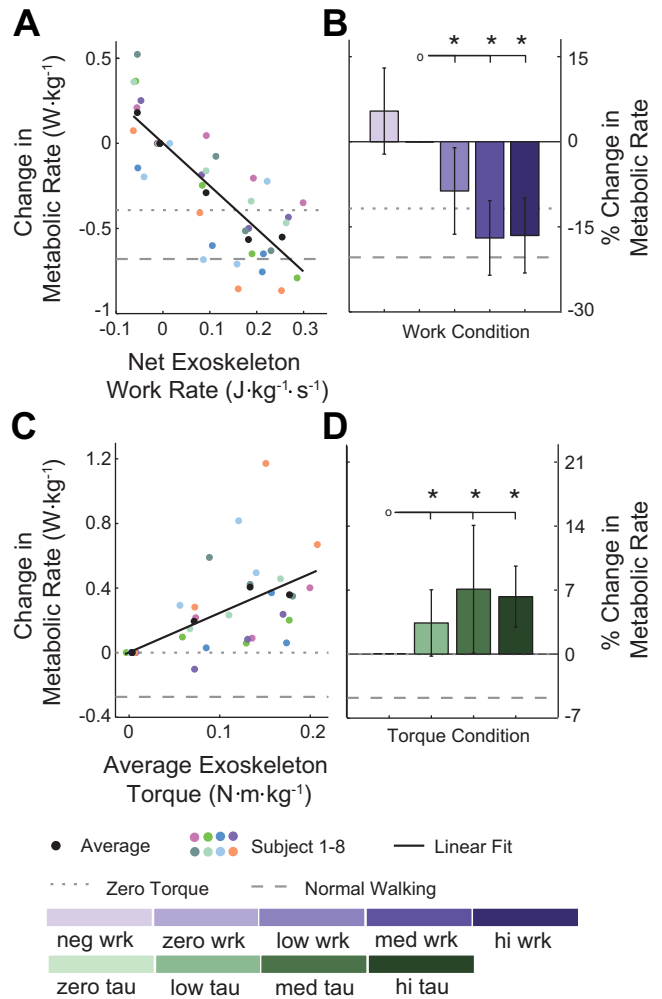


Fig. 5. Metabolic rate decreased with increasing exoskeleton work input, but increased with increasing exoskeleton torque support. A: change in metabolic rate from the Zero Work condition vs. net exoskeleton work rate. Colored dots represent individual subject data, black dots represent average data, and the solid black line is a linear fit. Dotted and dashed gray lines represent average metabolic rate for the Zero Torque and Normal Walking conditions, respectively. B: average change in metabolic rate across Work Study conditions. Darker purple indicates higher work conditions. Error-bars indicate intersubject variability. C: change in metabolic rate from the Zero Torque condition vs. average exoskeleton torque. Dotted and dashed gray lines represent average metabolic rate for the Zero Torque and Normal Walking conditions, respectively. D: average change in metabolic rate across Torque Study conditions. Darker green indicates higher torque conditions. Error-bars indicate intersubject variability. *Statistical significance with respect to the conditions designated by open circles.

decreased by 37% from the Zero Work condition to the High Work condition ($P = 0.02$, Fig. 6, A and B), while negative biological ankle work rate increased in magnitude by 22% from the Zero Work condition to the High Work condition ($P = 0.02$). Positive biological work rate decreased by 55% from the Zero Torque condition to the High Torque condition ($P = 1 \cdot 10^{-5}$), while negative biological work rate decreased in magnitude by 35% from the Zero Torque condition to the High Torque condition ($P = 9 \cdot 10^{-5}$). Biological ankle torque was reduced in the Work Study (ANOVA, $P = 0.02$; Fig. 6, C and D) and was substantially reduced in the Torque Study (ANOVA, $P = 7 \cdot 10^{-14}$).

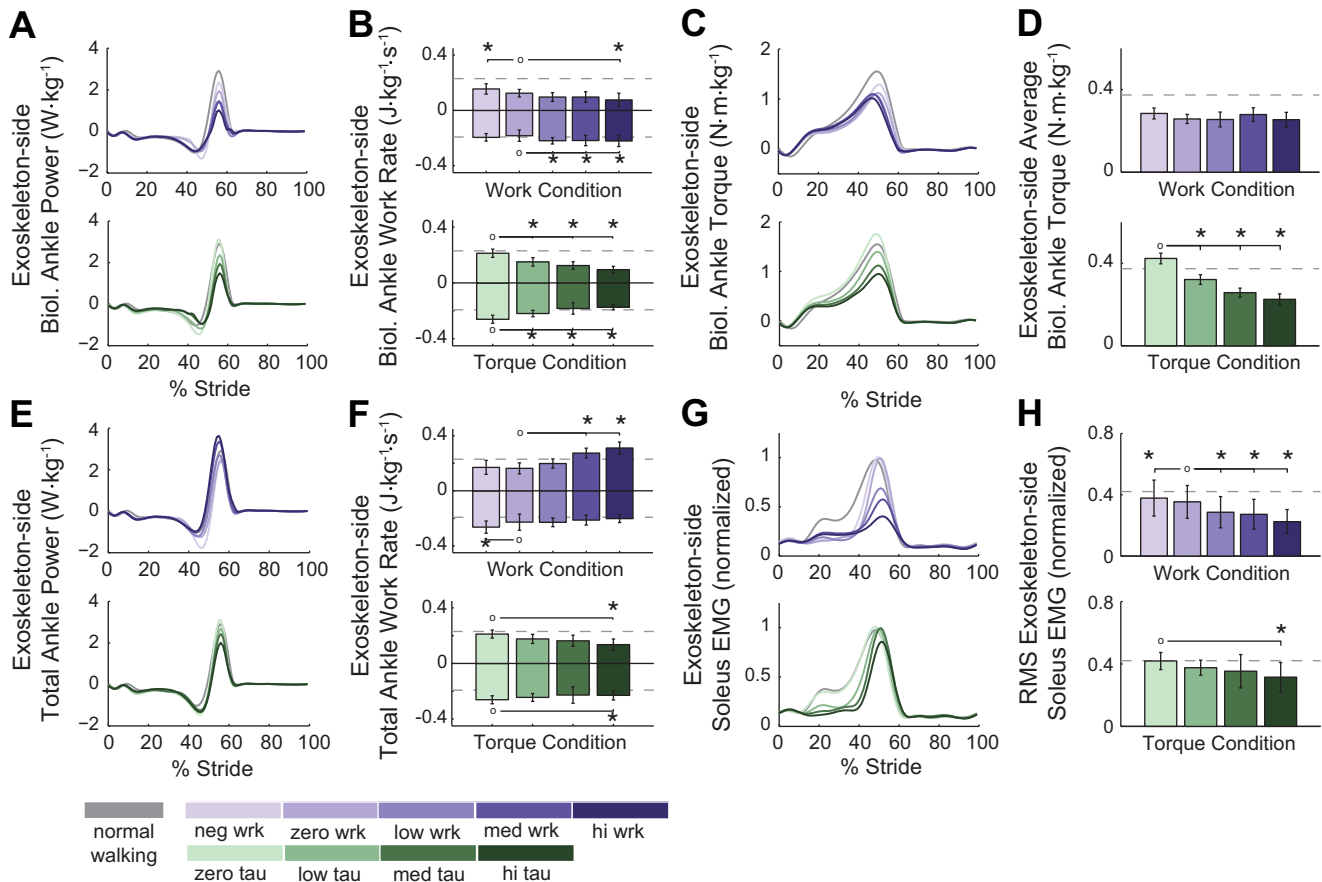


Fig. 6. Effort-related outcomes improved at the assisted ankle for both the Work Study and the Torque Study, while effects on total ankle work differed. *A*: biological power. *B*: biological work rate. *C*: biological torque. *D*: average biological torque. *E*: combined ankle power. *F*: combined ankle work rate. *G*: soleus EMG. *H*: root-mean-square (RMS) soleus EMG. Work Study is in purple, Torque Study is in green, and darker colors indicate higher values. Normal Walking is in gray. Curves are study average trajectories. Bars and whiskers are means \pm SD of subject-wise integration of corresponding curves. *Statistical significance with respect to the conditions designated by open circles.

Average biological torque decreased by 45% from the Zero Torque condition to the High Torque condition ($P = 2 \cdot 10^{-7}$). Normalized root-mean-square soleus muscle activity decreased by 37% from the Zero Work condition to the High Work condition ($P = 6 \cdot 10^{-5}$; Fig. 6, *G* and *H*) and decreased by 24% from the Zero Torque condition to the High Torque condition ($P = 2 \cdot 10^{-3}$).

Total exoskeleton-side ankle work increased with increasing exoskeleton work but decreased with increasing exoskeleton torque. Total positive ankle work rate increased by 94% from the Zero Work condition to the High Work condition ($P = 4 \cdot 10^{-5}$; Fig. 6, *E* and *F*). By contrast, total positive ankle work rate decreased by 33% from the Zero Torque condition to the High Torque condition ($P = 5 \cdot 10^{-3}$).

Center-of-Mass Mechanics

Increasing exoskeleton work increased exoskeleton-side center-of-mass push-off work and decreased contralateral-limb collision and rebound work, while increasing exoskeleton torque led to opposite trends in center-of-mass mechanics (Fig. 7). In the Work Study, exoskeleton-side push-off work increased, while contralateral-limb collision and rebound work decreased (ANOVA, $P = 2 \cdot 10^{-13}$, $P = 7 \cdot 10^{-4}$, and $P = 7 \cdot 10^{-5}$, respectively). Assisted-limb push-off work rate in-

creased by 44%, while contralateral-limb rebound work rate decreased by 73% from the Zero Work condition to the High Work condition ($P = 1 \cdot 10^{-6}$ and $P = 6 \cdot 10^{-3}$, respectively). In the Torque Study, exoskeleton-side push-off work decreased, while contralateral-limb collision and rebound work appeared to increase (ANOVA, $P = 4 \cdot 10^{-4}$, $P = 0.06$, and $P = 0.2$, respectively). Assisted-limb push-off work rate decreased by 19% from the Zero Torque condition to the High Torque condition ($P = 6 \cdot 10^{-3}$).

Contralateral-limb push-off work decreased and exoskeleton-side collision work increased across Work Study conditions (ANOVA, $P = 6 \cdot 10^{-5}$ and $P = 6 \cdot 10^{-4}$, respectively; see Fig. A9) but did not change across Torque Study conditions (ANOVA, $P = 0.5$ and $P = 0.1$, respectively). From the Zero Work condition to the High Work condition, contralateral-limb push-off work rate decreased by 11% and exoskeleton-side collision work rate increased by 31% ($P = 7 \cdot 10^{-4}$ and $P = 0.02$, respectively).

Contralateral Knee Mechanics

Increased net exoskeleton work led to reduced muscle activity and biological components of work and torque at the contralateral knee joint, while increased average exoskeleton torque had the opposite effect (Fig. 8). Negative and

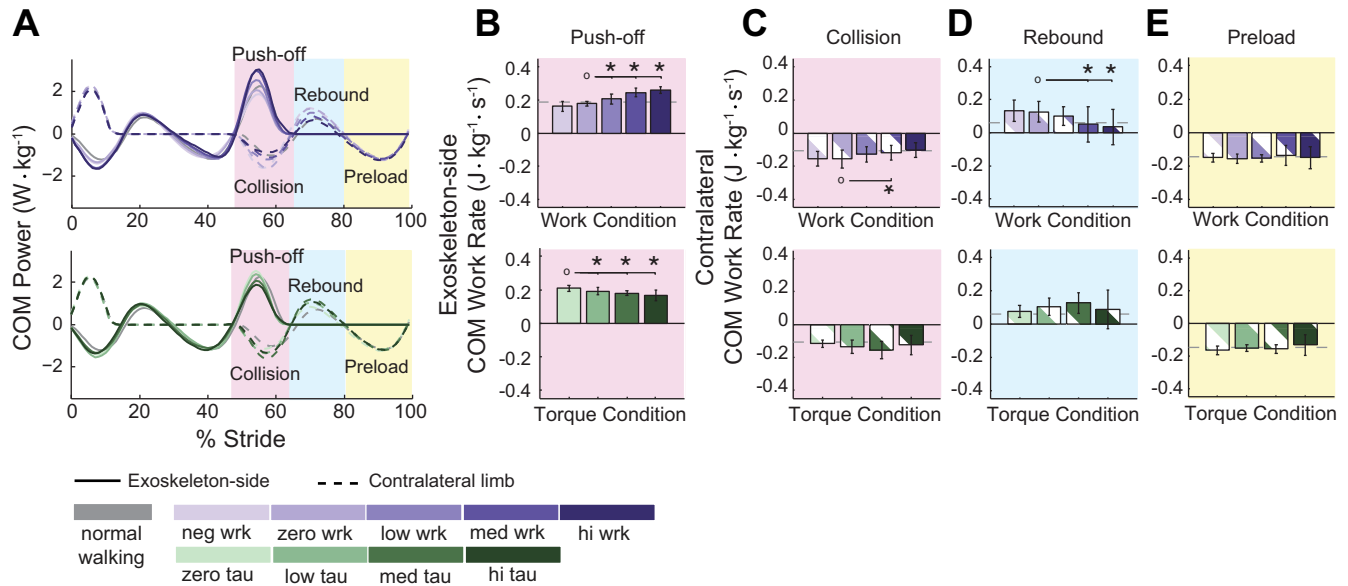


Fig. 7. In the Work Study, exoskeleton-side center-of-mass (COM) push-off work increased and contralateral-limb collision and rebound work decreased, while in the Torque Study opposite trends were observed. *A*: power. *B*: exoskeleton-side push-off work rate. *C*: contralateral-limb collision work rate. *D*: contralateral-limb rebound work rate. *E*: contralateral-limb preload work rate. Work rate is defined as the integral of power in the highlighted regions divided by stride time. Work Study is in purple, Torque Study is in green, and darker colors indicate higher values. Normal Walking is in gray. Curves are study-average trajectories, with exoskeleton-side power solid and contralateral-side power dashed. Bars and whiskers are means \pm SD of subject-wise integration of corresponding curves in the shaded regions, with exoskeleton-side bars solid and contralateral-side bars striped. The pink region corresponds to exoskeleton-side push-off and contralateral-limb collision, the blue region corresponds to contralateral-limb rebound, and the yellow region corresponds to contralateral-limb preload. *Statistical significance with respect to the conditions designated by open circles.

positive work rates, extension torque, and vastus muscle activity all decreased in magnitude with increasing exoskeleton work (ANOVA, $P = 2 \cdot 10^{-4}$, $P = 7 \cdot 10^{-7}$, $P = 6 \cdot 10^{-5}$, and $P = 0.02$, respectively) and increased with increasing exoskeleton torque (ANOVA, $P = 0.03$, $P = 0.01$, $P = 0.01$, and $P = 0.04$, respectively). From the Zero Work condition to the High Work condition, the magnitude of negative and positive contralateral knee work rate decreased by 44 and 48%, respectively ($P = 0.01$ and $P = 2 \cdot 10^{-3}$, respectively). From the Zero Work condition to the High Work condition, contralateral knee extension torque and vastus muscle activity decreased by 34 and 26%, respectively ($P = 5 \cdot 10^{-3}$ and $P = 0.01$, respectively).

Stride time was 1.16 ± 0.05 s in the Zero Torque condition and remained within 2% of this value across all conditions (ANOVA, $P = 0.2$). Kinematic and kinetic results for all lower-limb joints, muscle activity for all measured muscles, and center-of-mass work rates when the contralateral limb is trailing are shown in the APPENDIX. Complete numerical results are also presented in the APPENDIX (see Tables A1 and A2). A video of a subject walking in the different exoskeleton conditions is provided in the Supplementary Materials (Supplemental Material for this article is available online at the Journal website).

DISCUSSION

We conducted an experiment in which we explored the independent effects of a particular mode of work input and torque support on metabolic rate, center-of-mass mechanics, joint mechanics, and muscle activity. Metabolic energy consumption decreased with increasing exoskeleton work but, surprisingly, increased with increasing average exoskel-

eton torque. Both interventions reduced effort-related measures at the assisted joint, such as biological ankle work, biological ankle torque, and soleus muscle activity. Changes elsewhere in the body, arising from unexpected changes in human coordination, differed between interventions and seemed to best explain the observed trends in metabolic rate.

Metabolic energy consumption decreased with increasing exoskeleton work input. As expected, part of this reduction seems to have been a result of reduced effort at the assisted ankle joint. Net biological ankle joint work became increasingly negative across Work Study conditions, implying increasingly negative muscle work, which is less costly than isometric force production or positive muscle fascicle work at the same force (33). In addition, soleus muscle activity decreased with increasing work input (Fig. 6, *G* and *H*), even though peak biological ankle torque remained relatively constant (Fig. 6*C*). As exoskeleton work increased, biological ankle torque peaked and dropped off earlier in the stance period. This earlier onset of biological ankle torque dropoff may explain reduced soleus muscle activity during the latter part of stance, i.e., preceding push-off. Musculoskeletal models could be used to explore these ideas further.

Total exoskeleton-side ankle work increased across Work Study conditions. Increases in positive work supplied by the device outweighed reductions in biological work. Increased total ankle work led to an increase in exoskeleton-side center-of-mass push-off work and decreased contralateral-limb collision work and rebound work. These results are consistent with simple walking model predictions of the effect of push-off work on center-of-mass mechanics (29, 38). Decreased collision and rebound work seem to have been accompanied by changes in contralateral knee mechan-

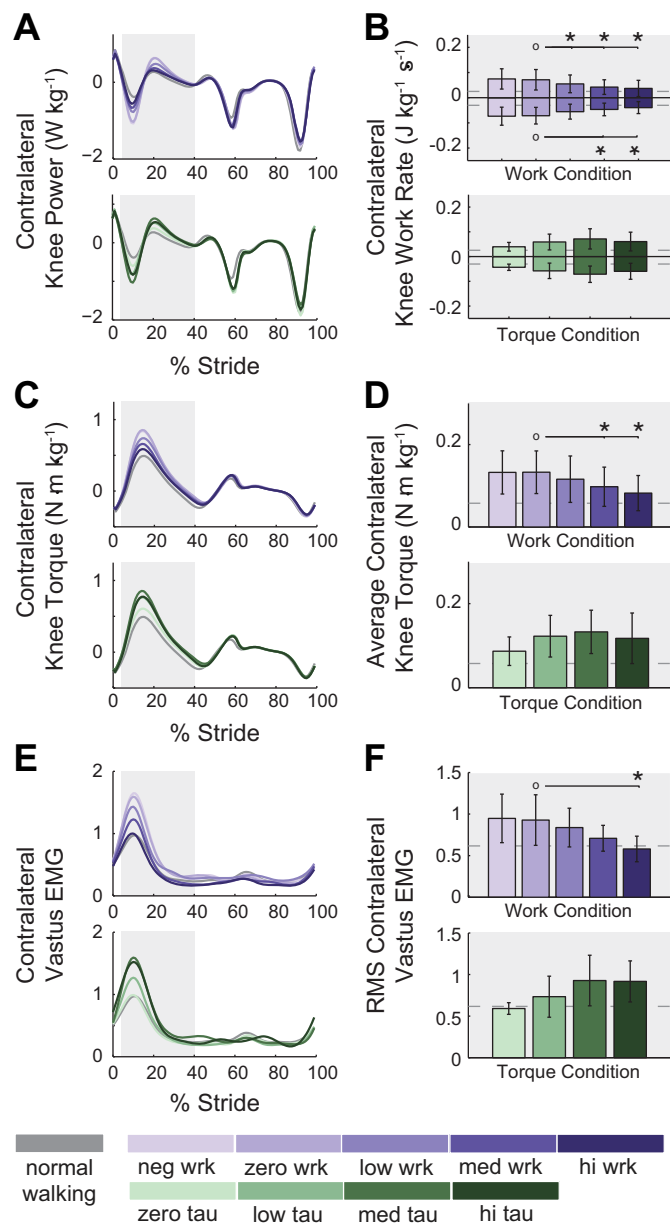


Fig. 8. Contralateral knee work, torque, and muscle activity decreased in the Work Study, while opposite trends were observed in the Torque Study. *A*: power. *B*: work rate. *C*: extension torque. *D*: average torque. *E*: vastus EMG. *F*: RMS vastus EMG. Work rate is defined as the integral of power in the highlighted region divided by stride time. Work Study is in purple, Torque Study is in green, and darker colors indicate higher values. Normal Walking is in gray. Curves are study-average trajectories. Bars and whiskers are means \pm SD of subject-wise integration of corresponding curves in the shaded region. *Statistical significance with respect to the conditions designated by open circles.

ics, seen as reduced work, extension torque, and vastus muscle activity around the step-to-step transition. Such changes may account for another substantial portion of the observed reduction in metabolic rate.

Contrary to our expectations, metabolic rate increased with increasing torque support of the described form. Despite large decreases in biological contributions to ankle torque and work, the reduction in energy use at the assisted ankle joint was likely relatively small given the small

decreases in plantarflexor muscle activity (Fig. 6, *G* and *H*). These small benefits were apparently outweighed by larger costs elsewhere in the body. The contralateral knee appears to be principally responsible for additional energy use, exhibiting increases in joint torque, joint work, and muscle activity with increasing average ankle exoskeleton torque.

Center-of-mass mechanics during the step-to-step transition may explain the coupling between activities of the trailing ankle and leading knee. Total ankle joint work decreased across Torque Study conditions and led to reduced center-of-mass push-off work. Simple walking models predict that reduced trailing limb push-off work disproportionately increases collision dissipation and rebound work in the leading leg (29, 38). Although this result has not always been observed in humans (e.g., Ref. 6), in this study increased torque support led to reduced total exoskeleton-side ankle push-off work and increased contralateral knee work during double-support. Alternatively, synergies between ankle plantarflexors and opposite-limb knee extensors, similar to the theorized coupling between stance-leg force and swing-leg afferent presynaptic inhibition (25), could explain how exoskeleton torques applied to the trailing ankle affected the contralateral knee. This interpretation must be tempered by recent findings suggesting limits in the ability of synergies to accurately capture neuromuscular control strategies (57). These ideas merit further exploration.

Subjects could have adapted to prevent the observed decrease in exoskeleton-side push-off work and corresponding increase in contralateral knee work in the Torque Study, but they did not. The decrease in biological ankle work is likely due to changes in muscle fascicle dynamics with increasing torque support, and the cost of maintaining consistent biological ankle work may have outweighed the potential benefits. During early and mid-stance, subjects reduced the biological component of ankle plantarflexion torque (Fig. 6, *C* and *D*), perhaps in an effort to maintain consistent total ankle torque (28). Lower biological ankle torque and soleus muscle activity during the first part of stance suggest that muscle-tendon force and Achilles tendon stretch were reduced leading into late stance. This result is similar to the observed reduction in muscle-tendon force and tendon stretch during hopping with a passive ankle exoskeleton (17). To provide the usual burst of positive push-off work, the calf muscles would have had to contract with higher velocity than normal, to either increase tension to normal levels by quickly stretching the Achilles tendon or increase contraction velocity beyond normal levels for the muscle-tendon unit as a whole. Muscle force per unit activation drops precipitously with increasing contraction velocity, meaning muscle activation would have had to increase substantially to generate normal levels of positive ankle work, incurring a large metabolic cost (48). This explanation is consistent with the lack of a large reduction in late-stance plantarflexor muscle activity and with the reduced ratio of biological joint torque to activation during the same period (Fig. 6, *C* and *G*). Increased plantarflexor muscle fascicle contraction velocity is also implicated by a greater change in fascicle length during push-off; with high exoskeleton torque, fascicle length at the onset of push-off was likely increased, since tendons stretched less but ankle

kinematics were consistent. These ideas merit further examination in a musculoskeletal model.

There are alternate explanations for the observed increase in metabolic rate with increased average exoskeleton torque. One possibility is that subjects did not learn to use the device effectively due to neurological constraints on patterns of muscle activation (39, 45, 56). This seems unlikely, because similar issues were not observed in the Work Study, but the idea is worth exploring more deeply in a neuromuscular model. Another explanation is coactivation of the tibialis anterior to counteract exoskeleton torque. While we did observe increased tibialis anterior muscle activity in some conditions (see Fig. A6), increases did not correlate well with increased metabolic rate.

The increase in metabolic rate with increasing average exoskeleton torque observed in this study would be difficult to predict using models that do not include muscles or models that assume fixed kinematics and kinetics. Simple dynamic walking models, for example, typically do not incorporate muscle dynamics and therefore would likely not have predicted the observed suppression of total ankle push-off work in the Torque Study. More complete skeletal models have been used to predict the effect of similar interventions (50). These models anticipated reduced torque and power from biological tissues at the assisted joints, consistent with our findings, but assumed fixed kinematics and kinetics and predicted reduced metabolic rate, which are inconsistent with results from this study. Similar difficulties would be encountered using more complete musculoskeletal models under the assumption of fixed kinetics and kinematics (2, 36, 40, 46), since the observed changes in metabolic rate were best explained by changes in whole body mechanics. Predictive simulations that optimize complete coordination patterns could overcome the above limitations (1, 43, 44). We expect the data from this study, and others with novel mechanical interventions, will help improve the predictive validity of such models (20).

With the aim of informing improved predictive models, we correlated several outcomes to metabolic rate and found that summed muscle activity fit observations better than joint work or center-of-mass work. It would be beneficial to have mechanical or electrical predictors of metabolic rate, which could be calculated in musculoskeletal models or measured more easily and at a higher frequency than whole body metabolic rate using respirometry. The sum of all positive and negative mechanical work on the center of mass, multiplied by muscle efficiencies, has been suggested as a determinant of metabolic cost in human walking (14, 30) but poorly fit observations in this study ($R^2 = 0.43$, $P = 0.08$; Fig. 9A), particularly across the Torque Study. The weighted sum of all positive and negative joint work has also previously been found to correlate well with metabolic rate (6), but also poorly fit observations in this study ($R^2 = 0.29$, $P = 0.16$; Fig. 9B), particularly for the Torque Study. It might be that work-related outcomes naturally tend to be more affected by work-related mechanical interventions or activities. The unweighted sum of all muscle activity measured by electromyography fit trends in both the Work Study and the Torque Study relatively well ($R^2 = 0.83$, $P = 0.002$; Fig. 9C), which is consistent with other findings (32, 42). This signal, or a refined version accounting for muscle

volume and maximum voluntary contraction, might be a candidate for online optimization in human locomotion experiments. Given the complexity of the physiological structures involved in human locomotion, however, it seems likely that this measure of muscle activity will not correlate to metabolic rate for some interventions.

Exoskeleton work assistance seems to reduce the energy cost of walking with more consistency than torque assistance. The finding that augmenting push-off work led to reduced metabolic rate is consistent with several recent studies (6, 9, 26, 31, 35, 41). Findings for spring-like torque support have been less consistent; metabolic rate has been reduced with some interventions (3, 11), while it was increased here and in other studies (51). Human-robot interactions, and their cascading dynamical consequences, are complex, and subtle differences between mechanical interventions can lead to substantial differences in the human response (8). We explored a narrow region of the space of possible torque support patterns; therefore, it is likely that more effective spring-like interventions exist. We also may not have provided participants with sufficient training and coaching, although this seems unlikely as these same results were observed in both naive and experienced participants. Nevertheless, it appears to be easier to obtain benefits from active exoskeletons than passive ones, at least in terms of metabolic energy use. This could mean that active elements should be incorporated into autonomous devices to obtain the greatest reductions in metabolic cost.

Exoskeleton work and torque were decomposed because of their potential relationships to the cost of performing net muscle work and the cost of producing muscle force, respectively. However, any separation of work and torque has inherent limitations due to the dependence of work on torque. Several potential decompositions of torque exist, including timing of torque application, peak torque, and average torque. Systematically changing net work while keeping one decomposition of torque constant across conditions, however, will result in changes in the other measures. For this study, average exoskeleton torque, or the integral of torque over a stride divided by stride time, was chosen as the torque parameter of interest because of its relevance to the cost of muscle force production; researchers have used the integral of muscle force, divided by body weight, as a measure of the metabolic cost of producing force with muscle (24). The effects of other decompositions of torque on biomechanical outcomes are interesting and should also be explored.

Work and torque were applied unilaterally in this experiment. In the Work Study, exoskeleton-side center-of-mass push-off work increased and contralateral-limb collision and rebound work decreased, while on the subsequent step contralateral-limb push-off work decreased and assisted-limb collision work increased, indicating an asymmetric gait pattern. Although asymmetric gait patterns are known to increase metabolic cost in some situations (13, 55), it is not known whether a symmetric gait is optimal given an asymmetric morphology. Metabolic energy consumption in the High Work condition was below the value in the Zero Torque condition, in which gait was more symmetric. This supports the idea that symmetric gait need not be optimal given an asymmetric system.

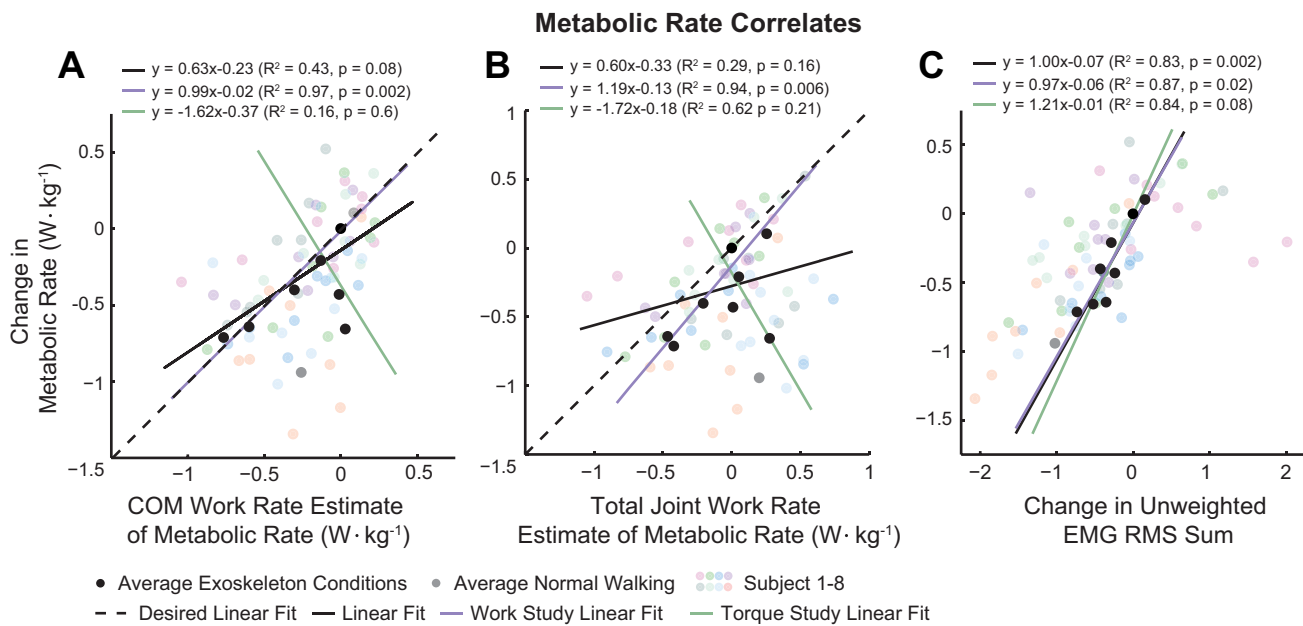


Fig. 9. Unweighted sum of measured EMG best correlated with changes in metabolic rate. *A*: measured metabolic rate vs. estimate of metabolic rate based on center-of-mass work. *B*: measured metabolic rate vs. estimated metabolic rate based on total joint work. *C*: measured metabolic rate vs. unweighted sum of the RMS of all measured muscle activity. Black dots represent average data for all conditions. Colored dots represent data for individual subjects. Dashed black line indicates the desired linear fit. Black, purple, and green solid lines are the linear fits to average data for all conditions, average Work Study data, and average Torque Study data, respectively.

Two participants had difficulty adapting to the exoskeleton behavior and were excluded as statistical outliers. This may have been due to insufficient training. Additional exposure to the exoskeleton, or coaching on its use, may have allowed participants to better interact with the exoskeleton. Desired exoskeleton torque and work values were normalized to body mass for each participant and enforced via iterative learning compensation. Thus, the applied torque trajectories were likely not optimal for individual participants. Optimizing exoskeleton torque trajectories for each participant could result in faster adaptation and more beneficial changes in biomechanical outcomes.

Conclusions

In this study, we independently varied a particular mode of exoskeleton work input and torque support over a large range and measured metabolic rate, center-of-mass mechanics, joint mechanics, and electromyography to characterize the human physiological response to these two interventions. We found that increasing this mode of exoskeleton work delivery reduced metabolic energy consumption, while increasing this mode of average exoskeleton torque support increased metabolic energy consumption. The observed trends in metabolic rate are best explained by disparate changes in total exoskeleton-side ankle mechanics, arising from interactions with muscle fascicle dynamics, and the cascading effects on whole body coordination, particularly at the contralateral knee. This result illustrates the difficulty in using very simple models or more complex models that assume fixed kinematics or kinetics to predict the impact of a mechanical intervention on a human. It supports the case for experimental approaches designed to measure the full

biomechanical response of the human to a wide variety of novel assistance strategies. We expect that the empirical data provided by this study will lead to improved predictive models of human coordination and to better designs of assistive devices.

APPENDIX: JOINT MECHANICS, MUSCLE ACTIVITY, AND CENTER-OF-MASS MECHANICS

Figures A1, A2, A3, A4, A5, A6, A7, A8, and A9 show joint mechanics, muscle activity, and center-of-mass mechanics. Tables A1 and A2 show all numerical results across the Work Study and Torque Study, respectively.

ACKNOWLEDGMENTS

We thank Anne Alcasid, Roberto Jaime, and Julie Rekant for assistance with data collection and processing, Joshua Caputo and Roberto Quesada for assistance with hardware maintenance, and Hartmut Geyer for use of data collection equipment.

GRANTS

This material is based on work supported by National Science Foundation Grant IIS-1355716 and Graduate Research Fellowship Grant DGE-1252552.

DISCLOSURES

No conflicts of interest, financial or otherwise, are declared by the author(s).

AUTHOR CONTRIBUTIONS

Author contributions: R.W.J. and S.H.C. conception and design of research; R.W.J. performed experiments; R.W.J. analyzed data; R.W.J. and S.H.C. interpreted results of experiments; R.W.J. prepared figures; R.W.J. drafted manuscript; R.W.J. and S.H.C. edited and revised manuscript; R.W.J. and S.H.C. approved final version of manuscript.

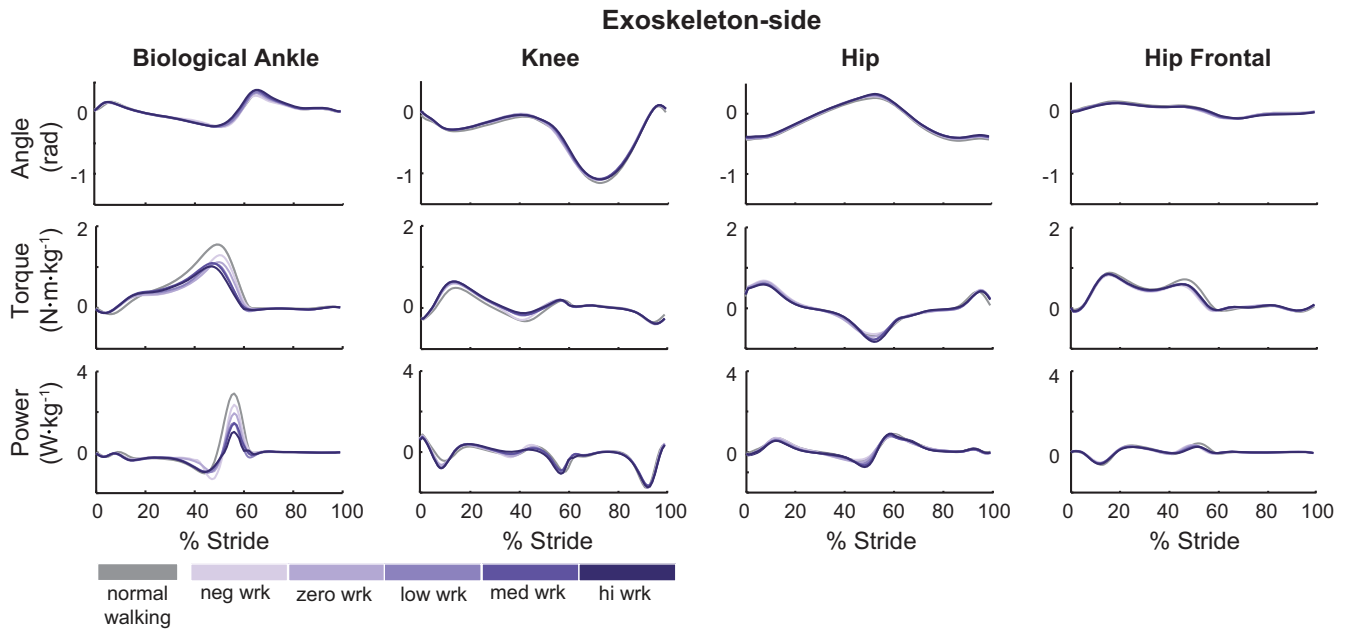


Fig. A1. Exoskeleton-side joint mechanics across Work Study conditions. The biological component of ankle torque and power decreased with increasing work, while other exoskeleton-side joint mechanics did not appear to change across conditions. Positive values indicate extension and negative values indicate flexion. Purple lines represent average trajectories with darker colors indicating higher work values.

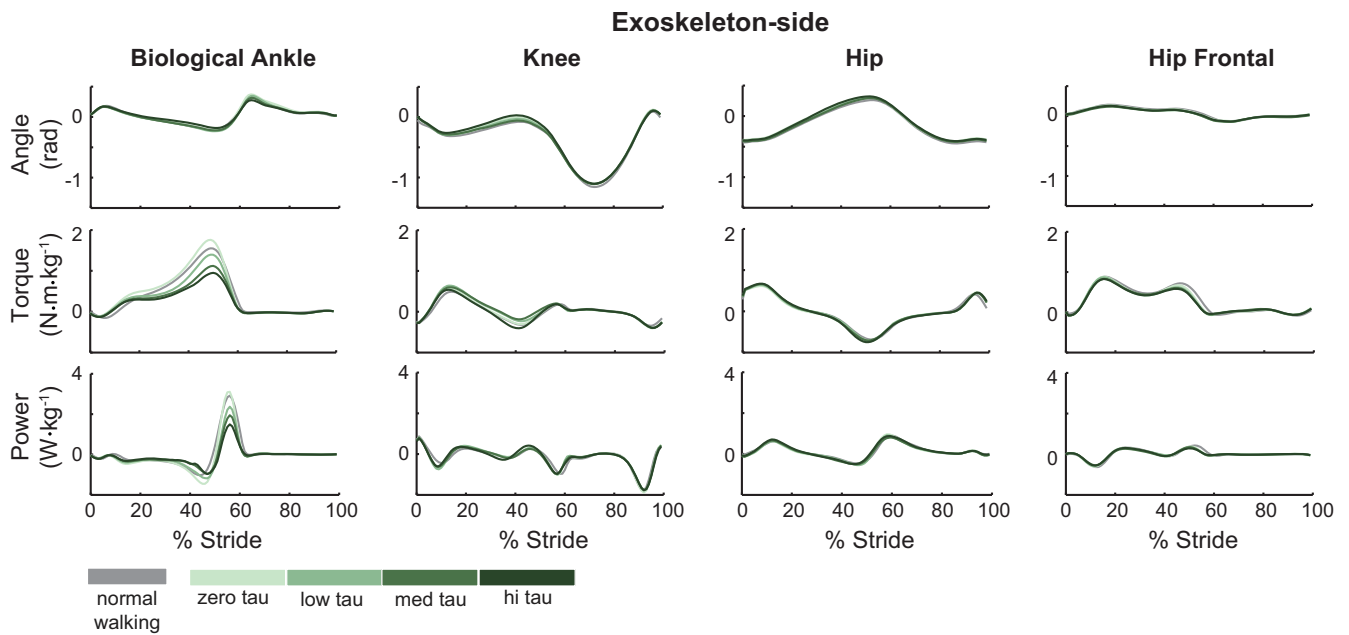


Fig. A2. Exoskeleton-side joint mechanics across Torque Study conditions. The biological component of ankle torque and power decreased with increasing torque, while other exoskeleton-side joint mechanics did not appear to change across conditions. Positive values indicate extension and negative values indicate flexion. Green lines represent average trajectories with darker colors indicating higher torque values.

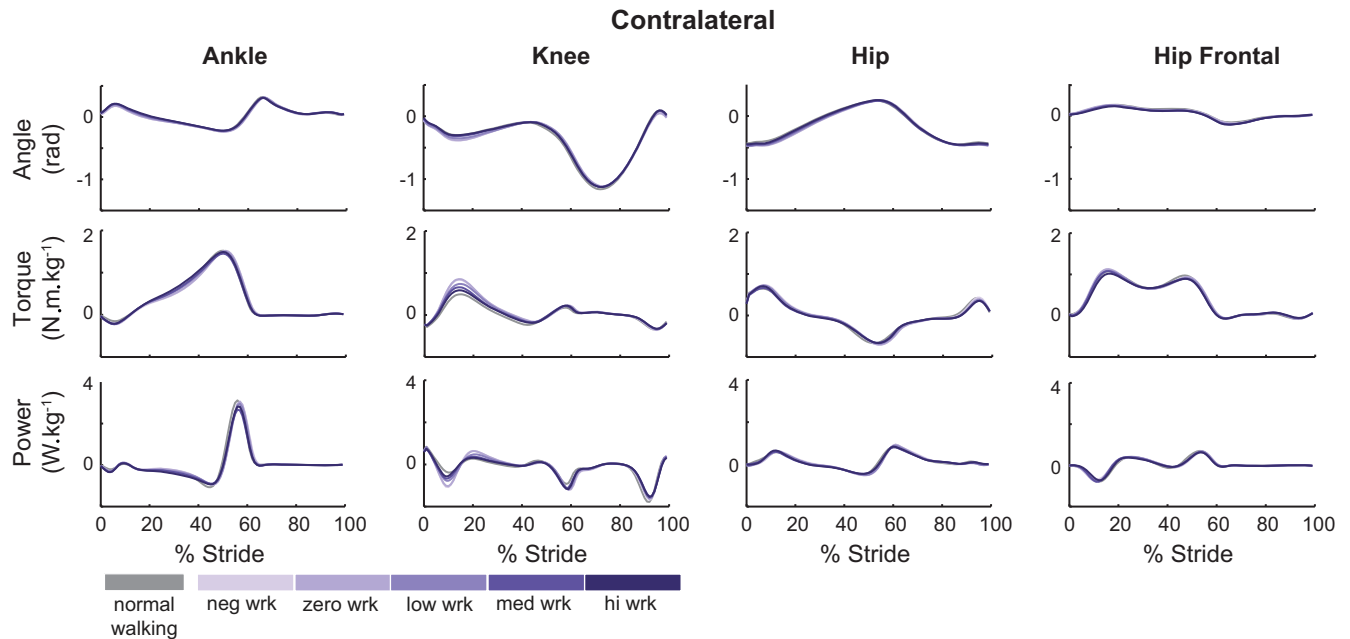


Fig. A3. Contralateral-limb joint mechanics across Work Study conditions. Knee torque and power decreased with increasing work, while other contralateral joint mechanics did not appear to change across conditions. Positive values indicate extension and negative values indicate flexion. Purple lines represent average trajectories with darker colors indicating higher work values.

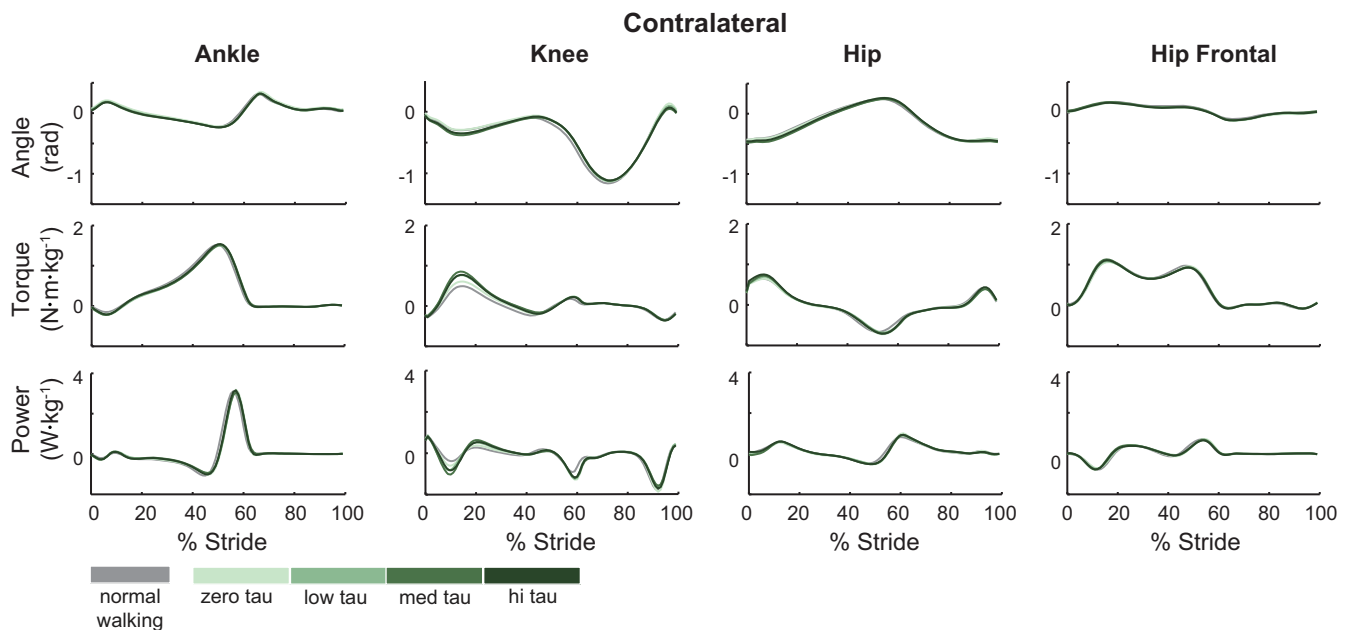


Fig. A4. Contralateral-limb joint mechanics across Torque Study conditions. Knee torque and power increased with increasing torque, while other contralateral joint mechanics did not appear to change across conditions. Positive values indicate extension and negative values indicate flexion. Green lines represent average trajectories with darker colors indicating higher torque values.

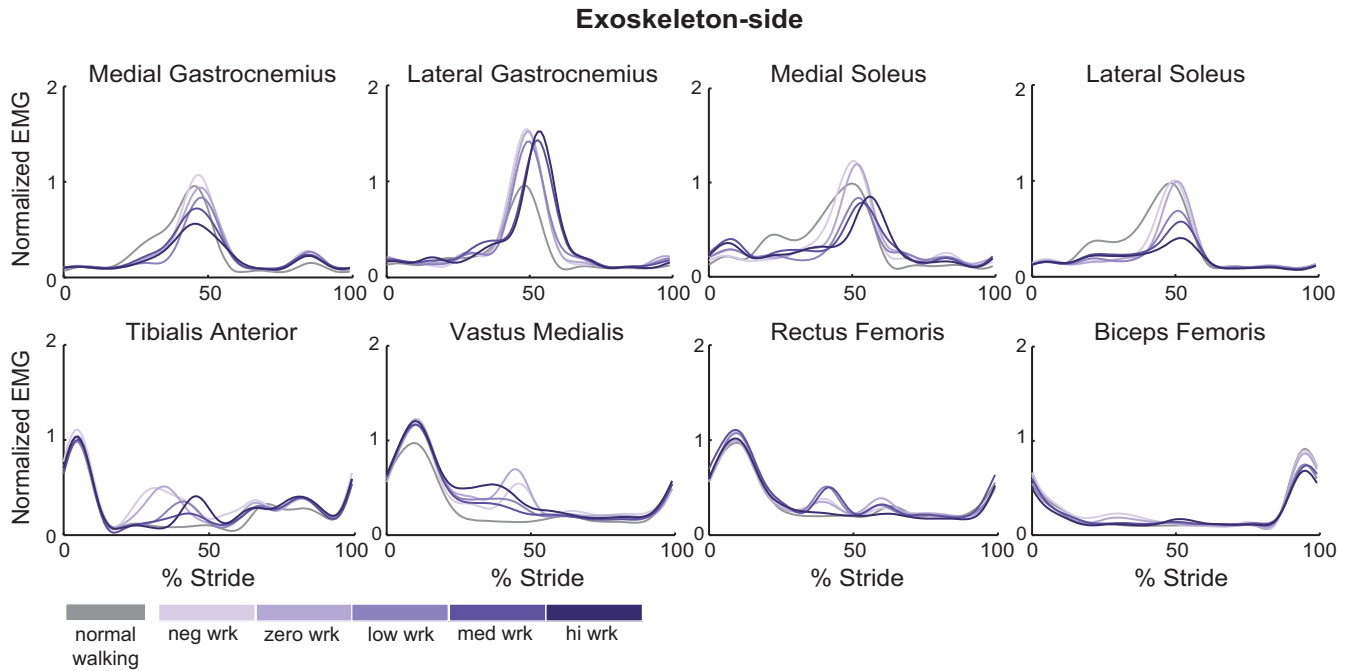


Fig. A5. Exoskeleton-side electromyography across Work Study conditions. Electromyographic signals were normalized to average peak activation during Normal Walking. Purple lines represent average trajectories with darker colors indicating higher work values.

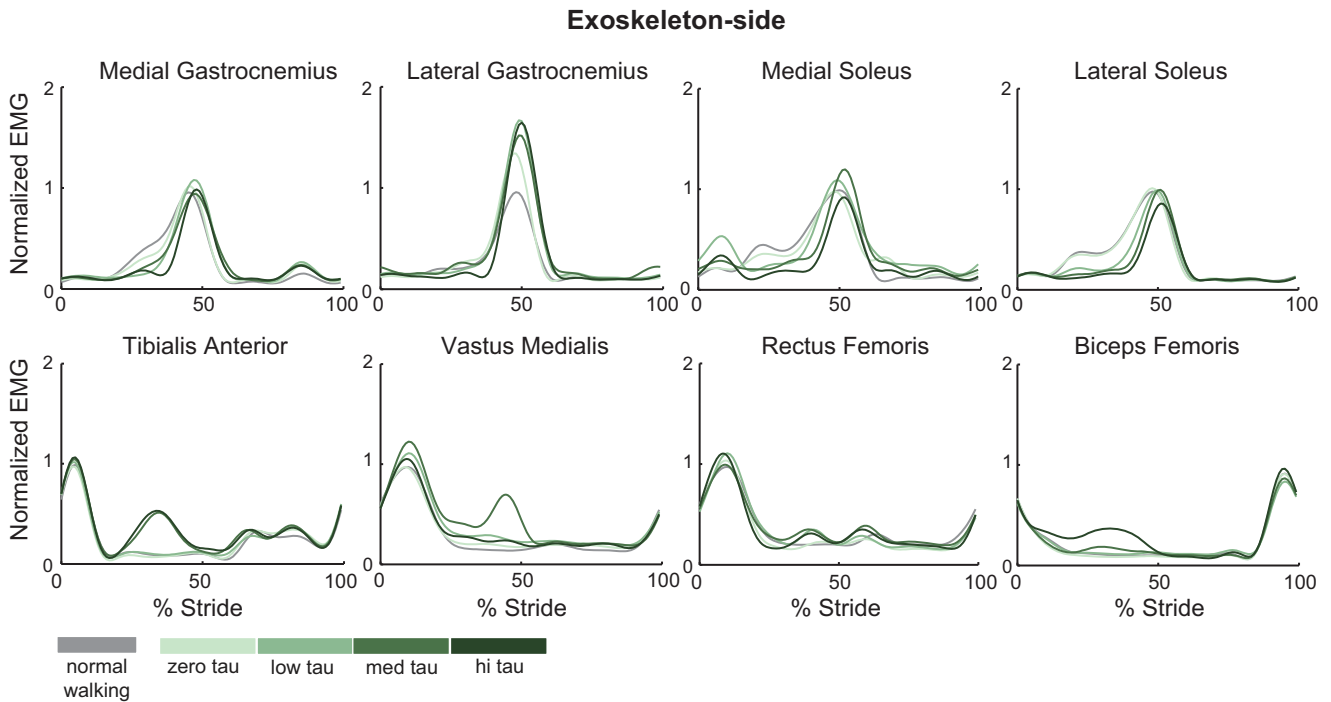


Fig. A6. Exoskeleton-side electromyography across Torque Study Conditions. Electromyographic signals were normalized to average peak activation during Normal Walking. Green lines represent average trajectories with darker colors indicating higher torque values.

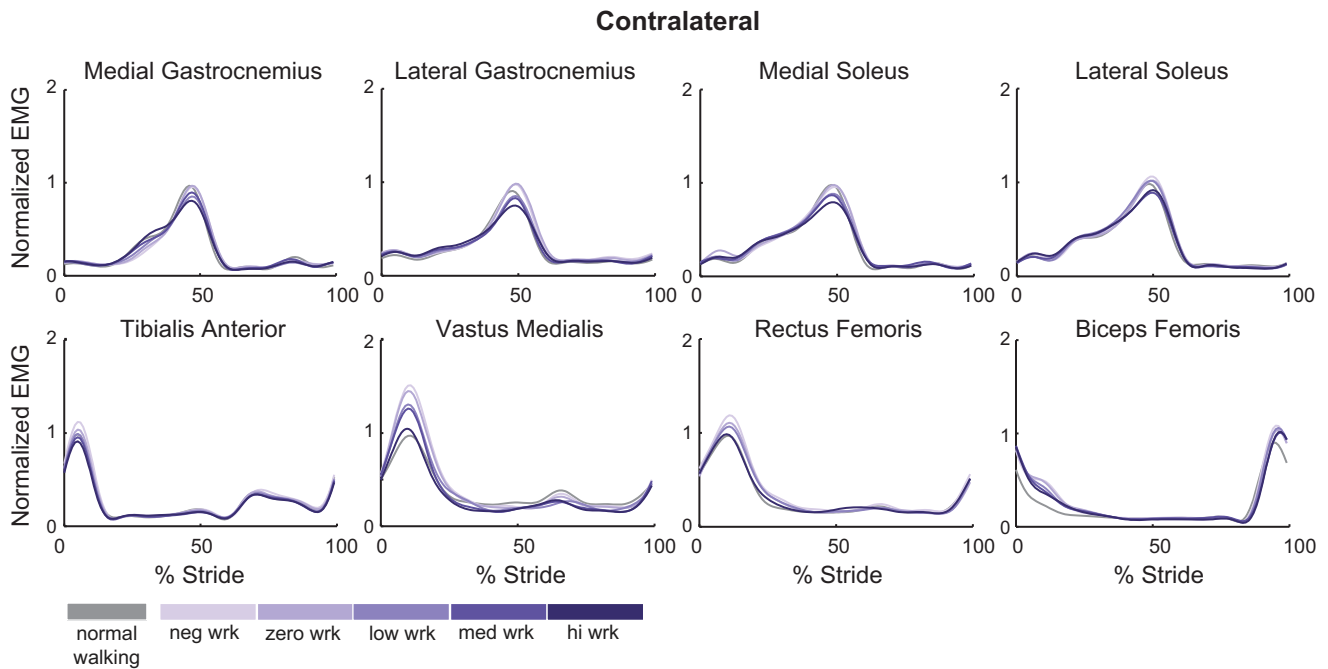


Fig. A7. Contralateral-limb electromyography across Work Study Conditions. Electromyographic signals were normalized to average peak activation during Normal Walking. Purple lines represent average trajectories with darker colors indicating higher work values.

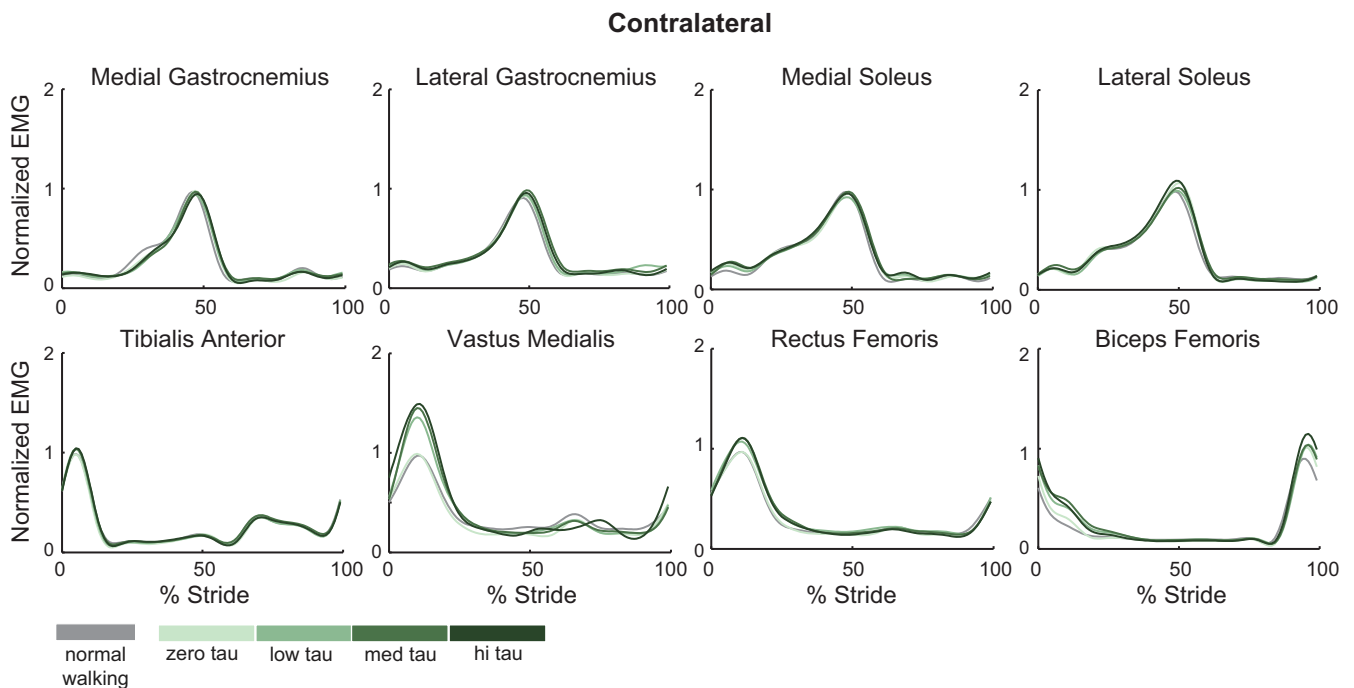


Fig. A8. Contralateral-limb electromyography across Torque Study Conditions. Electromyographic signals were normalized to average peak activation during Normal Walking. Green lines represent average trajectories with darker colors indicating higher torque values.

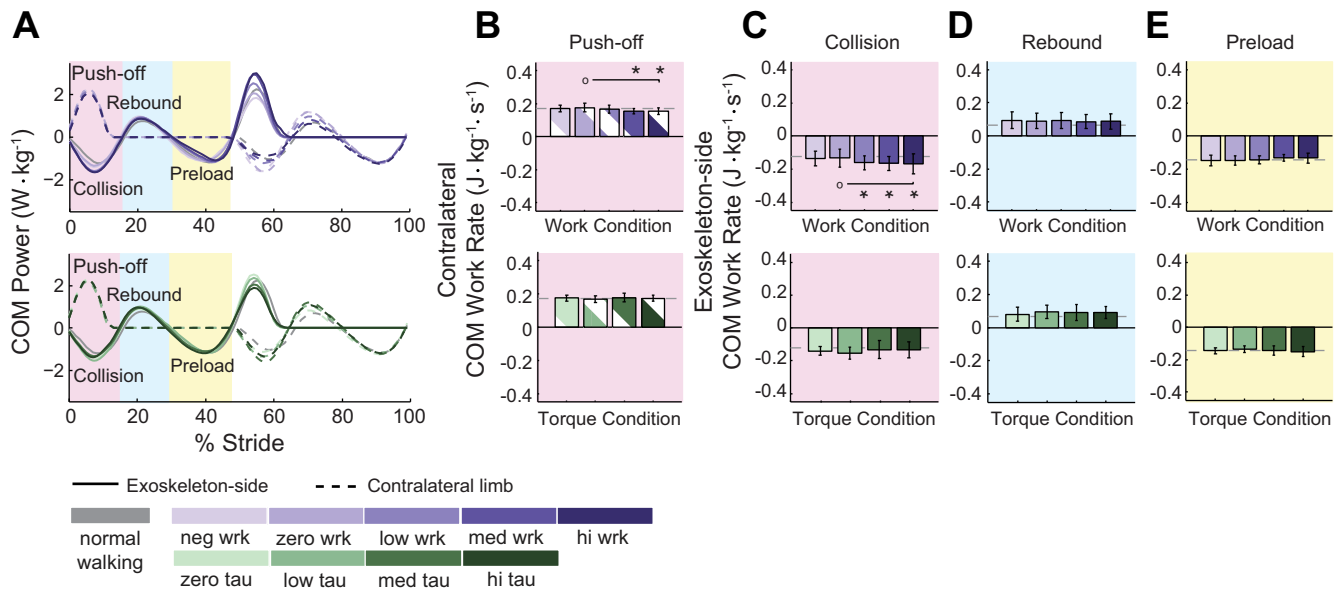


Fig. A9. In the Work Study, contralateral-limb center-of-mass push-off work decreased and exoskeleton-side collision work increased in magnitude, while in the Torque Study no trends were observed in center-of-mass mechanics when the contralateral limb was trailing. *A*: power. *B*: contralateral-limb push-off work rate. *C*: exoskeleton-side collision work rate. *D*: exoskeleton-side rebound work rate. *E*: exoskeleton-side preload work rate. Work rate is defined as the integral of power in the highlighted region divided by stride time. Work Study is in purple, Torque Study is in green, and darker colors indicate higher values. Normal Walking is in gray. Curves are study-average trajectories, with exoskeleton-side power solid and contralateral-side power dashed. Bars and whiskers are means \pm SD of subject-wise integration of corresponding curves in the shaded regions, with exoskeleton-side bars solid and contralateral-side bars striped. The pink region corresponds to contralateral-limb push-off and exoskeleton-side collision, the blue region corresponds to exoskeleton-side rebound, and the yellow region corresponds to exoskeleton-side preload. *Statistical significance with respect to the conditions designated by open circles.

Table A1. Work Study results

	Negative Work	Zero Work	Low Work	Medium Work	High Work
Net exoskeleton work rate, J·kg ⁻¹ ·s ⁻¹	-0.054 \pm 0.0076*	-0.0065 \pm 0.0088	0.092 \pm 0.012*	0.18 \pm 0.018*	0.25 \pm 0.030*
Average exoskeleton torque, N·m·kg ⁻¹	0.12 \pm 0.022	0.13 \pm 0.015	0.13 \pm 0.016	0.1 \pm 0.019	0.14 \pm 0.022
Change in metabolic rate, W/kg	0.18 \pm 0.25	0.00 \pm 0.00	-0.29 \pm 0.25*	-0.57 \pm 0.22*	-0.55 \pm 0.22*
Exoskeleton side					
Positive biol. ankle work rate, J·kg ⁻¹ ·s ⁻¹	0.16 \pm 0.037*	0.12 \pm 0.027	0.097 \pm 0.031	0.097 \pm 0.038	0.076 \pm 0.049*
Negative biol. ankle work rate, J·kg ⁻¹ ·s ⁻¹	-0.19 \pm 0.027	-0.18 \pm 0.041	-0.22 \pm 0.023*	-0.22 \pm 0.037*	-0.22 \pm 0.040*
Positive total ankle work rate, J·kg ⁻¹ ·s ⁻¹	0.17 \pm 0.051	0.16 \pm 0.040	0.20 \pm 0.034	0.27 \pm 0.035*	0.31 \pm 0.043*
Negative total ankle work rate, J·kg ⁻¹ ·s ⁻¹	-0.26 \pm 0.045	-0.23 \pm 0.059	-0.23 \pm 0.032	-0.21 \pm 0.036*	-0.20 \pm 0.028*
Biol. ankle torque, N·m·kg ⁻¹	0.28 \pm 0.026	0.26 \pm 0.022	0.26 \pm 0.036	0.28 \pm 0.033	0.25 \pm 0.036
RMS soleus EMG (normalized)	0.38 \pm 0.12*	0.35 \pm 0.11	0.29 \pm 0.10*	0.27 \pm 0.097*	0.22 \pm 0.079*
COM push-off work rate, J·kg ⁻¹ ·s ⁻¹	0.16 \pm 0.031	0.18 \pm 0.014	0.21 \pm 0.030*	0.25 \pm 0.027*	0.26 \pm 0.022*
COM collision work rate, J·kg ⁻¹ ·s ⁻¹	-0.14 \pm 0.045	-0.13 \pm 0.054	-0.16 \pm 0.043	-0.16 \pm 0.041*	-0.17 \pm 0.060*
Contralateral					
COM push-off work rate, J·kg ⁻¹ ·s ⁻¹	0.17 \pm 0.021	0.18 \pm 0.025	0.17 \pm 0.024*	0.15 \pm 0.016*	0.16 \pm 0.019*
COM collision work rate, J·kg ⁻¹ ·s ⁻¹	-0.16 \pm 0.044	-0.16 \pm 0.054	-0.13 \pm 0.046	-0.12 \pm 0.044*	-0.10 \pm 0.044
COM rebound work rate, J·kg ⁻¹ ·s ⁻¹	0.13 \pm 0.064	0.13 \pm 0.063	0.10 \pm 0.057	0.051 \pm 0.11*	0.035 \pm 0.11*
Positive knee work rate, J·kg ⁻¹ ·s ⁻¹	0.075 \pm 0.040	0.071 \pm 0.041	0.055 \pm 0.035*	0.042 \pm 0.029*	0.037 \pm 0.032*
Negative knee work rate, J·kg ⁻¹ ·s ⁻¹	-0.073 \pm 0.036	-0.072 \pm 0.033	-0.056 \pm 0.030*	-0.047 \pm 0.025*	-0.040 \pm 0.024*
Knee extension torque, N·m·kg ⁻¹	0.14 \pm 0.048	0.14 \pm 0.046	0.12 \pm 0.051*	0.11 \pm 0.041*	0.093 \pm 0.038*
RMS vastus EMG (normalized)	1.24 \pm 0.29	1.19 \pm 0.26	1.09 \pm 0.25*	1.05 \pm 0.20*	0.88 \pm 0.17*

COM, center of mass; RMS, root-mean-squares. *Statistical significance with respect to the Zero Work condition.

Table A2. Torque Study results

	Zero Torque	Low Torque	Medium Torque	High Torque
Net exoskeleton work rate, J·kg ⁻¹ ·s ⁻¹	-0.0027 ± 0.0022	-0.0003 ± 0.0064	-0.0065 ± 0.0088	-0.016 ± 0.0059*
Average exoskeleton torque, N·m·kg ⁻¹	0.0032 ± 0.0033	0.072 ± 0.011*	0.13 ± 0.015*	0.18 ± 0.021*
Change in metabolic rate, W/kg	0.00 ± 0.00	0.19 ± 0.21*	0.41 ± 0.40*	0.36 ± 0.19*
Exoskeleton side				
Positive biol. ankle work rate, J·kg ⁻¹ ·s ⁻¹	0.21 ± 0.029	0.15 ± 0.031*	0.12 ± 0.027*	0.095 ± 0.024*
Negative biol. ankle work rate, J·kg ⁻¹ ·s ⁻¹	-0.26 ± 0.029	-0.22 ± 0.024*	-0.18 ± 0.041*	-0.17 ± 0.019*
Positive total ankle work rate, J·kg ⁻¹ ·s ⁻¹	0.21 ± 0.029	0.18 ± 0.033	0.16 ± 0.040	0.14 ± 0.040*
Negative total ankle work rate, J·kg ⁻¹ ·s ⁻¹	-0.26 ± 0.029	-0.25 ± 0.028	-0.23 ± 0.059	-0.23 ± 0.034*
Biol. ankle torque, N·m·kg ⁻¹	0.42 ± 0.026	0.32 ± 0.024*	0.26 ± 0.022*	0.23 ± 0.026*
RMS soleus EMG (normalized)	0.42 ± 0.055	0.38 ± 0.049	0.35 ± 0.11	0.32 ± 0.094*
COM push-off work rate, J·kg ⁻¹ ·s ⁻¹	0.21 ± 0.018	0.19 ± 0.020*	0.18 ± 0.014*	0.17 ± 0.034*
COM collision work rate, J·kg ⁻¹ ·s ⁻¹	-0.14 ± 0.026	-0.15 ± 0.035	-0.13 ± 0.054	-0.13 ± 0.048
Contralateral				
COM push-off work rate, J·kg ⁻¹ ·s ⁻¹	0.17 ± 0.019	0.17 ± 0.021	0.18 ± 0.025	0.17 ± 0.019
COM collision work rate, J·kg ⁻¹ ·s ⁻¹	-0.12 ± 0.022	-0.14 ± 0.039	-0.16 ± 0.054	-0.13 ± 0.058
COM rebound work rate, J·kg ⁻¹ ·s ⁻¹	0.077 ± 0.036	0.10 ± 0.053	0.13 ± 0.063	0.088 ± 0.12
Positive knee work rate, J·kg ⁻¹ ·s ⁻¹	0.039 ± 0.018	0.059 ± 0.032	0.071 ± 0.041	0.060 ± 0.038
Negative knee work rate, J·kg ⁻¹ ·s ⁻¹	-0.043 ± 0.013	-0.058 ± 0.031	-0.072 ± 0.033	-0.060 ± 0.032
Knee extension torque, N·m·kg ⁻¹	0.098 ± 0.027	0.13 ± 0.047	0.14 ± 0.046	0.13 ± 0.055
RMS vastus EMG (normalized)	0.86 ± 0.071	1.12 ± 0.32	1.19 ± 0.26	1.29 ± 0.39

*Statistical significance with respect to Zero Torque condition.

REFERENCES

- Ackermann M, van den Bogert AJ. Optimality principles for model-based prediction of human gait. *J Biomech* 43: 1055–1060, 2010.
- Anderson FC, Pandy MG. Dynamic optimization of human walking. *J Biomech Eng* 123: 381–390, 2001.
- Bregman DJ, Harlaar J, Meskers CG, de Groot V. Spring-like ankle foot orthoses reduce the energy cost of walking by taking over ankle work. *Gait Post* 35: 148–153, 2012.
- Brockway JM. Derivation of formulae used to calculate energy expenditure in man. *Hum Nutr Clin Nutr* 41C: 463–471, 1987.
- Browning RC, Modica JR, Kram R, Goswami A. The effects of adding mass to the legs on the energetics and biomechanics of walking. *Med Sci Sports Exerc* 39: 515–525, 2007.
- Caputo JM, Collins SH. Prosthetic ankle push-off work reduces metabolic rate but not collision work in non-amputee walking. *Sci Rep* 4: 7213, 2014.
- Caputo JM, Collins SH. A universal ankle-foot prosthesis emulator for experiments during human locomotion. *J Biomech Eng* 136: 035002, 2014.
- Collins SH. What do walking humans want from mechatronics? (Invited Presentation). In: *International Conference on Mechatronics*. Vicenza, Italy: IEEE, 2013, p. 24–27, 2013.
- Collins SH, Jackson RW. A method for harnessing least-effort drives in robotic locomotion training. In: *Proceedings of International Conference on Rehabilitation Robotics*. Seattle, WA: IEEE, 2013, p. 1–6.
- Collins SH, Kuo AD. Recycling energy to restore impaired ankle function during human walking. *PLoS One* 5: e9307, 2010.
- Collins SH, Wiggin MB, Sawicki GS. Reducing the energy cost of human walking using an unpowered exoskeleton. *Nature* 522: 212–215, 2015.
- de Leva P. Adjustments to Zatsiorsky-Seluyanov's segment inertia parameters. *J Biomech* 29: 1223–1230, 1996.
- Detrembleur C, Dierick F, Stoquart G, Chantaine F, Lejune T. Energy cost, mechanical work, and efficiency of hemiparetic walking. *Gait Post* 18: 47–55, 2003.
- Donelan JM, Kram R, Kuo AD. Mechanical work for step-to-step transitions is a major determinant of the metabolic cost of human walking. *J Exp Biol* 205: 3717–3727, 2002.
- Donelan JM, Kram R, Kuo AD. Simultaneous positive and negative external mechanical work in human walking. *J Biomech* 35: 117–124, 2002.
- Drillis R, Contini R, Bluestein M. Body segment parameters: a survey of measurement techniques. *Artificial Limbs* 25: 44–66, 1964.
- Farris DJ, Robertson BD, Sawicki GS. Elastic ankle exoskeletons reduce soleus muscle force but not work in human hopping. *J Appl Physiol* 115: 579–585, 2013.
- Ferris DP, Gordon KE, Sawicki GS. An improved powered ankle-foot orthosis using proportional myoelectric control. *Gait Post* 23: 425–428, 2006.
- Ferris DP, Sawicki GS, Domingo AR. Powered lower limb orthoses for gait rehabilitation. *Top Spinal Cord Inj Rehab* 11: 34–49, 2005.
- Fregly BJ, Besier TF, Lloyd DG, Delp SL, Banks SA, Pandy MG, D'Lima DD. Grand challenge competition to predict in vivo knee loads. *J Orthop Res* 30: 503–513, 2012.
- Glantz SA. *Primer of Biostatistics*. New York: McGraw-Hill Medical, 2012, p. 65–67.
- Gordon KE, Ferris DP, Kuo AD. Metabolic and mechanical energy costs of reducing vertical center of mass movement during gait. *Arch Phys Med Rehabil* 90: 136–144, 2009.
- Grabowski A, Farley CT, Kram R. Independent metabolic costs of supporting body weight and accelerating body mass during walking. *J Appl Physiol* 98: 579–583, 2005.
- Griffin TM, Roberts TJ, Kram R. Metabolic cost of generating muscular force in human walking: insights from load-carrying and speed experiments. *J Appl Physiol* 95: 172–183, 2003.
- Hayes HB, Chang YH, Hochman S. Stance-phase force on the opposite limb dictates swing-phase afferent presynaptic inhibition during locomotion. *J Neurophysiol* 107: 3168–3180, 2012.
- Herr HM, Grabowski AM. Bionic ankle-foot prosthesis normalizes walking gait for persons with leg amputation. *Proc Roy Soc Lon B* 279: 457–464, 2012.
- Hitt J, Oymagil AM, Sugar T, Hollander K, Boehler A, Fleeger J. Dynamically controlled ankle-foot orthosis (DCO) with regenerative kinetics: incrementally attaining user portability. In: *Proceeding of International Conference on Robotics and Automation*. Roma, Italy: IEEE, 2007, p. 1541–1546.
- Kao P, Lewis CL, Ferris DP. Invariant ankle moment patterns when walking with and without a robotic ankle exoskeleton. *J Biomech* 43: 203–209, 2010.
- Kuo AD. A simple model predicts the step length-speed relationship in human walking. *J Biomech Eng* 123: 264–269, 2001.
- Kuo AD, Donelan JM, Ruina A. Energetic consequences of walking like an inverted pendulum: step-to-step transitions. *Exerc Sport Sci Rev* 33: 88–97, 2005.
- Malcolm P, Derave W, Galle S, De Clercq D. A simple exoskeleton that assists plantarflexion can reduce the metabolic cost of human walking. *PLoS One* 8: e56137, 2013.
- Marsh AP, Martin PE. Effect of cycling experience, aerobic power, and power output on preferred and most economical cycling cadences. *Med Sci Sports Exerc* 29: 1225–1232, 1997.
- McMahon TA. *Muscles, Reflexes, Locomotion*. Princeton, NJ: Princeton Univ. Press, 1984, p. 34–35.
- Meinders M, Gitter A, Czernieckie JM. The role of ankle plantar flexor muscle work during walking. *Scand J Rehabil Med* 30: 39–46, 1998.

35. **Mooney LM, Rouse EJ, Herr HM.** Autonomous exoskeleton reduces metabolic cost of human walking during load carriage. *J Neuroeng Rehabil* 11: 80, 2014.
36. **Neptune RR, Kautz SA, Zajac FE.** Contributions of the individual ankle plantar flexors to support, forward progression and swing initiation during walking. *J Biomech* 34: 1387–1398, 2001.
37. **Roberts TJ, Marsh RL, Weyand PG, Taylor CR.** Muscular force in running turkeys: the economy of minimizing work. *Science* 257: 1113–1115, 1997.
38. **Ruina A, Bertram JE, Srinivasan M.** A collision model of the energetic cost of support work qualitatively explains leg sequencing in walking and galloping, pseudo-elastic leg behavior in running and the walk-to-run transition. *J Theor Biol* 237: 170–192, 2005.
39. **Safavynia SA, Torres-Oviedo G, Ting LH.** Muscle synergies: implications for clinical evaluation and rehabilitation of movement. *Top Spinal Cord Inj Rehabil* 17: 16–24, 2011.
40. **Sartori M, Reggiani M, Farina D, Lloyd DG.** EMG-driven forward-dynamic estimation of muscle force and joint moment about multiple degrees of freedom in the human lower extremity. *PLoS One* 7: 1–11, 2012.
41. **Sawicki GS, Ferris DP.** Mechanics and energetics of level walking with powered ankle exoskeletons. *J Exp Biol* 211: 1402–1413, 2008.
42. **Silder A, Besier T, Delp SL.** Predicting the metabolic cost of incline walking from muscle activity and walking mechanics. *J Biomech* 45: 1842–1849, 2012.
43. **Song S, Geyer H.** Generalization of a muscle-reflex control model to 3D walking. In: *Proceedings of International Conference on Engineering in Medicine and Biology Society*. Osaka, Japan: IEEE, 2013, p. 7463–7466.
44. **Srinivasan S, Westervelt ER, Hansen AH.** A low-dimensional sagittal-plane forward-dynamic model for asymmetric gait and its application to study the gait of transtibial prosthesis users. *J Biomech Eng* 131: 031003, 2009.
45. **Steele KM, Tresch MC, Perreault EJ.** The number and choice of muscles impact the results of muscle synergy analyses. *Front Comp Neurosci* 7: 105, 2013.
46. **Thelen DG, Anderson FC.** Using computed muscle control to generate forward dynamic simulations of human walking from experimental data. *J Biomech* 39: 1107–1115, 2006.
47. **Umberger BR.** Stance and swing phase costs in human walking. *J Roy Soc Int* 7: 1329–1340, 2010.
48. **Umberger BR, Gerritsen KGM, Martin PE.** A model of human muscle energy expenditure. *Comput Methods Biomech Biomed Eng* 6: 99–111, 2003.
49. **Umberger BR, Rubenson J.** Understanding muscle energetics in locomotion: New modeling and experimental approaches. *Exerc Sport Sci Rev* 39: 59–67, 2011.
50. **van den Bogert AJ.** Exotendons for assistance of human locomotion. *Biomed Eng Online* 2: 17, 2003.
51. **van Dijk W, van der Kooij H, Hekman E.** A passive exoskeleton with artificial tendons: design and experimental evaluation. In: *Proceedings of International Conference on Robotics and Automation*. Zurich, Switzerland: IEEE, 2011, p. 1–6.
52. **Wiggin MB, Sawicki GS, Collins SH.** Apparatus and Clutch for Using Controlled Storage and Release of Mechanical Energy to Aid Locomotion (Provisional Patent). *United States Patent Office*, 2012, 13/586, 528.
53. **Winter DA.** *Biomechanics and Motor Control of Human Movement*. Toronto, Canada: Wiley, 1990, p. 107–138.
54. **Witte KA, Zhang J, Jackson RW, Collins SH.** Design of two lightweight, high-bandwidth torque controlled ankle exoskeletons. In: *Proceedings of International Conference on Robotics and Automation*. Seattle, WA: IEEE, 2015.
55. **Wutzke CJ, Sawicki GS, Lewek MD.** The influence of a unilateral fixed ankle on metabolic and mechanical demands. *J Biomech* 45: 2405–2410, 2012.
56. **Yen JT, Auyang AG, Chang YH.** Joint-level kinetic redundancy is exploited to control limb-level forces during human hopping. *Exp Brain Res* 196: 439–451, 2009.
57. **Zelik KE, La Scaleia V, Ivanenko YP, Lacquaniti F.** Can modular strategies simplify neural control of multidirectional human locomotion? *J Neurophysiol* 111: 1686–1702, 2014.
58. **Zhang J, Cheah CC, Collins SH.** Experimental comparison of torque control methods on an ankle exoskeleton during human walking. In: *Proceedings of International Conference on Robotics and Automation*. Seattle, WA: IEEE, 2015.